The Design and Assembly of Neural Circuits for Vocal Communication in Songbirds

ARCHIVES

MASSACHUSETTS INSTITUTE OF TECHNOLOGY
JUN 0 4 2009
LIBRARIES

by

Benjamin Barnett Scott

A.B. Biology

University of Chicago, 2001

SUBMITTED TO THE DEPARTMENT OF BRAIN AND COGNITIVE SCIENCES IN PARTIAL FULFILLMENT OF THE REQUIREMENTS FOR THE DEGREE OF

DOCTOR OF PHILOSOPHY IN NEUROSCIENCE

AT THE MASSACHUSETTS INSTITUTE OF TECHNOLOGY

JUNE 2009

The author hereby grants to MIT permission to reproduce and to distribute publicly paper and electronic copies of this thesis document in whole or in part in any medium now known or hereafter created.

Signature of the Author_____
Benjamin Scott

Certified by_____
Carlos Lois, M.D., Ph.D.
Assistant Professor of Neuroscience
Thesis Supervisor

Accepted by_____
Earl Miller, Ph.D.
Picower Professor of Neuroscience
Chairman, Department Committee for Graduate Students

Contents

Abstract

Unlike the human brain, which produces few neurons in adulthood, the brains of songbirds continue to produce new neurons throughout life. The function of these new neurons is not know, although it has been suggested that they endow the avian brain with a remarkable regenerative capacity that does not exist in mammals. It has also been proposed that the addition of new neurons in adulthood underlies behavioral plasticity, such as song learning. A better understanding of the cellular mechanisms that control the addition of new neurons to the postnatal brain may help clarify its biological function. This thesis is an investigation of the cell biology of postnatal neurogenesis in the songbird forebrain, with special emphasis on the High Vocal Center.

Neuronal progenitors in the juvenile zebra finch brain were identified by fate mapping using engineered retroviruses. Multiple populations of neural progenitors appear to exist in the juvenile zebra finch brain, and each produces different types of neurons. At least three cell types appear to be added to the postnatal finch brain. Homology between neurogenesis in the postnatal finch and embryonic mammalian forebrain was also assessed.

To characterize the mechanism of cell addition, videos were made, documenting the migration and integration of new neurons into the High Vocal Center. Neural progenitors were labeled using retroviruses, carrying the gene for the green fluorescent protein, allowing new neurons to be observed in the intact brain, with a powerful infrared laser. By replacing a small hole in the skull with a piece of optical glass, one could observe labeled neurons periodically over many days as they were born until they wired up to the existing circuitry. New neurons engaged in a previously undescribed form of migration. Further study of this form of neuron migration as well as other aspects of postnatal neurogenesis may lead to the development of strategies for replacing neurons in the human brain lost to death or disease.

Chapter 1

Introduction

All vertebrate species studied add new neurons to the brain throughout the lifetime of the animal. Since its discovery[1], postnatal neurogenesis has attracted significant attention because it stood in direct contrast to earlier dogma established by the classical neuroanatomists and it suggested that new neurons could be used to repair the human brain. Yet for all the attention this phenomenon has received in the past four decades, its biological function remains unknown.

The extent of postnatal neurogenesis varies by neuronal type and by species. In most species only a subset of neurons are added to the adult brain, with the remainder born during embryonic development. For example, mammals, including humans, add only two types of cells to the adult brain: the granule cells of the dentate gyrus and the granule cells of the olfactory bulb[2]. All other neurons are born shortly after birth. Neurogenesis is more widespread in other vertebrate species such as reptiles, birds, amphibians and fish (Kaslin et al., 2008). These observations raise the following questions: Why are some cell types replaced and not others? Why are some neuron types replaced in some animals and not replaced in others?

It has been hypothesized that neurogenesis plays a role in brain repair after traumatic injury or in tissue maintenance. However studies from songbirds have suggested an alternative hypothesis about the biological role of postnatal neurogenesis.

---

[1] In the early 1960s Josef Altman and colleagues at the Massachusetts Institute of Technology used tritiated thymidine to label newborn neurons in the brain (Altman, 1962). Tritiated thymidine gets incorporated into newly synthesized DNA and can be detected with radiographic film (Taylor et al., 1957) thus allowing dividing cells to be identified (Hughes et al., 1958). A central theme in this thesis is to highlight how technological developments lead to shifts in the intellectual landscape.

[2] It was Altman, who, working in mice, identified the limits of neurogenesis in the postnatal mammalian forebrain. New neurons were restricted to two zones, the olfactory bulb (Altman, 1969), which processes the sense of smell and the dentate gyrus (Altman, 1965), a region involved in the formation of new memories.

Major insight into the function of neurogenesis was obtained from studies in songbirds by Fernando Nottebohm and colleagues at the Rockefeller University. Like other avian species, songbirds exhibit robust neurogenesis throughout adulthood. Nottebohm and colleagues were particularly interested in the addition of new neurons to the song system, a specialized forebrain circuit that controls vocal communication. These studies were the first to document, by electrophysiological recordings (Paton and Nottebohm, 1984) and electron microscopy, that newborn neurons join the existing circuitry, making synapses with older resident neurons. In particular, one nucleus in the song system, the High Vocal Center (HVC), became the focus of research. In two songbird species, zebra finches and canaries, the highest rate of neurogenesis in HVC occurs during the critical period for song learning (Alvarez-Buylla et al., 1988; Nordeen and Nordeen, 1988). This observation has lead to the hypothesis that the postnatal neurogenesis may be a mechanism for behavior plasticity.

Canaries breed seasonally and in the spring the lengthening day leads to an increase of circulating testosterone in males, which in turn leads to increased territoriality and courtship behavior. Singing behavior, which is used to defend territory and attract mates, increases in frequency. In early spring canaries make modifications to their songs by adding and removing new syllables. At this time HVC swells in size (Nottebohm, 1981) due to the enlargement of existing neurons and the addition of new neurons. After the breeding period, many of the newborn neurons added during the spring undergo cell death, only to be replaced in the spring by new neurons (Alvarez-Buylla and Kirn, 1997). One interpretation of this replacement program is that the addition of a new cohort of spring neurons and loss of old cells is a mechanism for the formation of the new motor memories (Alvarez-Buylla et al., 1990). Although this hypothesis remains controversial, increased rates of neurogenesis have been observed to correlate with learning in other systems such as the hippocampus.

Only by manipulation of postnatal neurogenesis will we be able to test hypotheses about its biological function. Identification of the genes and cellular mechanisms of postnatal

neurogenesis will give us the tools to manipulate this process. Once we gain control we may be able to harness postnatal neurogenesis for brain repair.

Before attacking this problem it will be useful to consider separately the phases of life of a single neuron; proliferation (when and where cells are born), migration (how cells find and get integrated into neural circuits) and differentiation (what type of neurons these cells become).

Our first step in understanding postnatal neurogenesis is to characterize neuron proliferation. We want to know when and where neurons are born. This knowledge is required if we want to fully explain the biology of neurogenesis and will allow us to gain experimental control over new neurons. We can use our understanding of neurogenesis to genetically manipulate the new neurons selectively. Specific classes of cells can be manipulated genetically, if 1) there exists a known promoter for these cells or 2) a vector can be specifically targeted to these cells. Since tools for songbird transgenesis are only beginning to be developed (see Appendix) and promoters for cell type specific expression have not been described[3], we are better served to use vectors to deliver genes to directly to the cells of interest.

Retroviruses are particularly useful tools for delivering genes to proliferating cells (Figure 1). Two classes of retroviruses, lentiviruses[4] and oncoretroviruses, have been widely used for gene delivery to animal cells. Oncoretroviruses were the first retroviruses to be discovered (Coffin et al., 1997) and domesticated (Shimotohno and Temin, 1981). Domesticated oncoretroviruses, called oncoretroviral vectors, are produced in the laboratory and lack the ability to replicate and cause disease (but see (Hacein-Bey-Abina et al., 2003)). These vectors have been used for cell lineage analysis in the nervous system (Price et al., 1987; Turner and Cepko, 1987). Oncoretroviral

[3] No cis-acting DNA regulatory elements for songbird neurons have been identified.
[4] Vectors derived from lentiviruses will be discussed later on in the appendix.

vectors have been useful for the study of development because they can label cells genetically and they can be engineered to carry genes that encode protein markers, such as GFP and LacZ, allowing infected cells and all their progeny to be visually identified.

A second useful feature of oncoretroviral vectors is that they only infect actively dividing cells. Oncoretroviruses and their vectors require that the host cell undergo passage through mitosis for infection (Roe et al., 1993). It is believed that these cells require the breakdown of the envelope of the nuclear membrane to gain access to the host chromosomes. This requirement makes oncoretroviral vectors particularly useful when studying postnatal neurogenesis since oncoretroviral vectors can only infect actively dividing stem cells and are unable to infect post-mitotic neurons.

The necessary first step in using oncoretroviral vectors is to identify when and where new neurons are born. Based on experiments with tritiated thymidine it was hypothesized that new neurons were born from radial glia in the walls of the lateral ventricle. However, specific classes of neurons are born from different populations of radial glia that reside in separate locations along the wall of the lateral ventricle. Therefore it is possible, by targeting viral injection into these different areas to preferentially infect newborn neurons of specific subclasses. By systematically injecting oncoretroviral vectors carrying the gene for GFP in different locations throughout the LV and examining the spread of cells, I identified the positions that give rise to the neurons of the song system (Chapter 2).

Cells move by three primary mechanisms (Bray, 2001), 1) actively by propulsion or locomotion, examples include certain are single celled eukaryotes such as paramecium, bacteria, such as E. coli[5] and certain specialized metazoan cells such as sperm, 2) cells may move as a result of being pushed by other cells during growth. 3) cells may move actively by crawling. This later process describes how most neurons move and is

[5] This form of migration was thoroughly studied in E coli in the 1970s and represents the most satisfying body of work on migration from a theoretical perspective (Berg, 1975).

essential for proper formation of the vertebrate brain. Neurons are born from stem cells that lie within the ventricular zone (VZ) and must travel, sometimes over great distances, in order to reach their ultimate position within the brain. In humans, disruption of the genes that direct neuronal migration can cause severe mental retardation or death (Gleeson and Walsh, 2000). Since the failure of neurons to properly migrate carries serious consequences for the organism and this process is under tight genetic control.

How this neuron migration is regulated in the postnatal brain is not known. In other systems, such as the developing cerebral cortex, both chemical and electrical cues have been implicated in the regulation of neuron migration. Chemical cues may be presented locally or by diffusion. There is also mounting evidence of the influence of neurotransmitters (Komuro and Rakic, 1993; Manent et al., 2005). Cellular scaffolds also regulate neuron migration. In the developing vertebrate brain, radial fibers (the long projections of radial glia) form a substrate for the migration of neurons away from the VZ and into the brain. In mammals radial glia undergo apoptosis or differentiate into astrocytes after they serve their function as a migratory scaffold, however in birds, radial glia, persist into adulthood. In histological sections from the songbird brain, some new neurons appear to migrate along radial fibers, suggesting that radial glia may play a role in neuron migration in the adult brain. However, some areas of the songbird forebrain that receive new neurons do not contain radial glia, suggesting that other mechanisms of migration may exist.

Additional mechanisms may be necessary because the amount of extracellular space dramatically reduces as the brain matures (Bondareff and Narotzky, 1972). The high density of cells and neuropil with synapses that are stable for months to years (Holtmaat et al., 2005) suggests that the mature brain poses unique obstacles for migration, where the radial scaffold no longer exists and mature neurons and neuropil present an impediment to directed migration. One failure of neuron replacement strategies is the lack of migration observed in cells grafted into the mature brain. Perhaps a specialized genetic program exists for the migration of neurons through the mature brain. Activation

of this program may allow grafted cells to migrate through the adult brain to replace cells lost to death as they do in the avian brain (Scharff et al., 2000).

One strategy for gaining further insight into migration in the postnatal brain is to observe this process from cell birth through migration to differentiation. Observation of cell behavior, sometimes called cellular ethology, reveals a great deal about the rules that govern neurogenesis and provides a framework for the discovery of its molecular mechanisms (Lichtman and Smith, 2008; Schroeder, 2008). Recently it has become possible to monitor fluorescently labeled cells in vivo using two-photon microscopy[6]. These techniques have led to a revolution in cellular ethology and our understanding of development. In the following chapters I describe the behavior of new neurons during learning in the juvenile male zebra finch. Chapter 2 describes the origin of new neurons that join the song system, and describes a technique for genetically labeling specific subpopulations of new neurons. Chapter 3 describes the search-like behavior of newborn neurons as they integrate into the HVC. In Chapter 4, I speculate about the broader significance of these findings in relation to the evolution of behavioral traits and developmental origin of complex patterns in biological systems.

[6] The history of cell biology is inexorably linked with technical advances in microscopy. Once the light microscope was introduced to biology in the mid17th century, scientists began to observe small globular structures, "Cells" as the English scientists Robert Hooke described them (Hooke, 1667). By the mid 19th century, cells, and their ubiquitous nuclei had been observed in histological sections from plant and animal tissue. In 1839, Schwann and Schleiden formulated the basic tenets of what would become cell theory: cells form the basic units of life, the tissues of plants and animals are made up of cells (Schwann et al., 1847).

REFERENCES

Altman, J. (1962). Are new neurons formed in the brains of adult mammals? Science *135*, 1127-1128.
Altman, J. (1969). Autoradiographic and histological studies of postnatal neurogenesis. IV. Cell proliferation and migration in the anterior forebrain, with special reference to persisting neurogenesis in the olfactory bulb. J Comp Neurol *137*, 433-457.
Altman, J., and Das, G.D. (1965). Autoradiographic and histological evidence of postnatal hippocampal neurogenesis in rats. J Comp Neurol *124*, 319-335.
Alvarez-Buylla, A., and Kirn, J.R. (1997). Birth, migration, incorporation, and death of vocal control neurons in adult songbirds. J Neurobiol *33*, 585-601.
Alvarez-Buylla, A., Kirn, J.R., and Nottebohm, F. (1990). Birth of projection neurons in adult avian brain may be related to perceptual or motor learning. Science *249*, 1444-1446.
Alvarez-Buylla, A., Theelen, M., and Nottebohm, F. (1988). Birth of projection neurons in the higher vocal center of the canary forebrain before, during, and after song learning. Proc Natl Acad Sci U S A *85*, 8722-8726.
Berg, H. (1975). Bacterial Behavior. Nature *254*, 389-392.
Bondareff, W., and Narotzky, R. (1972). Age changes in the neuronal microenvironment. Science *176*, 1135-1136.
Bray, D. (2001). Cell movements : from molecules to motility, 2nd edn (New York: Garland Pub.).
Coffin, J.M., Hughes, S.H., and Varmus, H. (1997). Retroviruses (Plainview, N.Y.: Cold Spring Harbor Laboratory Press).
Gleeson, J.G., and Walsh, C.A. (2000). Neuronal migration disorders: from genetic diseases to developmental mechanisms. Trends Neurosci *23*, 352-359.
Hacein-Bey-Abina, S., Von Kalle, C., Schmidt, M., McCormack, M.P., Wulffraat, N., Leboulch, P., Lim, A., Osborne, C.S., Pawliuk, R., Morillon, E., *et al.* (2003). LMO2-associated clonal T cell proliferation in two patients after gene therapy for SCID-X1. Science *302*, 415-419.
Holtmaat, A.J., Trachtenberg, J.T., Wilbrecht, L., Shepherd, G.M., Zhang, X., Knott, G.W., and Svoboda, K. (2005). Transient and persistent dendritic spines in the neocortex in vivo. Neuron *45*, 279-291.
Hooke, R. (1667). Micrographia; or, Some physiological descriptions of minute bodies made by magnifying glasses. With observations and inquiries thereupon (London,: James Allestry [and John Martyn]).
Hughes, W.L., Bond, V.P., Brecher, G., Cronkite, E.P., Painter, R.B., Quastler, H., and Sherman, F.G. (1958). Cellular Proliferation in the Mouse as Revealed by Autoradiography with Tritiated Thymidine. Proc Natl Acad Sci U S A *44*, 476-483.
Kaslin, J., Ganz, J., and Brand, M. (2008). Proliferation, neurogenesis and regeneration in the non-mammalian vertebrate brain. Philos Trans R Soc Lond B Biol Sci *363*, 101-122.
Komuro, H., and Rakic, P. (1993). Modulation of neuronal migration by NMDA receptors. Science *260*, 95-97.
Lichtman, J.W., and Smith, S.J. (2008). Seeing circuits assemble. Neuron *60*, 441-448.

Manent, J.B., Demarque, M., Jorquera, I., Pellegrino, C., Ben-Ari, Y., Aniksztejn, L., and Represa, A. (2005). A noncanonical release of GABA and glutamate modulates neuronal migration. J Neurosci *25*, 4755-4765.
Nordeen, K.W., and Nordeen, E.J. (1988). Projection neurons within a vocal motor pathway are born during song learning in zebra finches. Nature *334*, 149-151.
Nottebohm, F. (1981). A brain for all seasons: cyclical anatomical changes in song control nuclei of the canary brain. Science *214*, 1368-1370.
Paton, J.A., and Nottebohm, F.N. (1984). Neurons generated in the adult brain are recruited into functional circuits. Science *225*, 1046-1048.
Price, J., Turner, D., and Cepko, C. (1987). Lineage analysis in the vertebrate nervous system by retrovirus-mediated gene transfer. Proc Natl Acad Sci U S A *84*, 156-160.
Roe, T., Reynolds, T.C., Yu, G., and Brown, P.O. (1993). Integration of murine leukemia virus DNA depends on mitosis. EMBO J *12*, 2099-2108.
Scharff, C., Kirn, J.R., Grossman, M., Macklis, J.D., and Nottebohm, F. (2000). Targeted neuronal death affects neuronal replacement and vocal behavior in adult songbirds. Neuron *25*, 481-492.
Schroeder, T. (2008). Imaging stem-cell-driven regeneration in mammals. Nature *453*, 345-351.
Schwann, T., Smith, H., Schleiden, M.J., Westleys & Clark, and Sydenham Society. (1847). Microscopical researches into the accordance in the structure and growth of animals and plants (London: Printed for the Sydenham Society).
Shimotohno, K., and Temin, H.M. (1981). Formation of infectious progeny virus after insertion of herpes simplex thymidine kinase gene into DNA of an avian retrovirus. Cell *26*, 67-77.
Taylor, J.H., Woods, P.S., and Hughes, W.L. (1957). The Organization and Duplication of Chromosomes as Revealed by Autoradiographic Studies Using Tritium-Labeled Thymidinee. Proc Natl Acad Sci U S A *43*, 122-128.
Turner, D.L., and Cepko, C.L. (1987). A common progenitor for neurons and glia persists in rat retina late in development. Nature *328*, 131-136.

Chapter 2

Developmental Origin and Identity of Song System Neurons Born During Vocal Learning in Songbirds

Attributions.

This chapter was previously published as:

Scott, B.B., and Lois, C. (2007). Developmental origin and identity of song system neurons born during vocal learning in songbirds. Journal of Comparative Neurology *502*, 202-214.

THE JOURNAL OF COMPARATIVE NEUROLOGY 502:202–214 (2007)

Developmental Origin and Identity of Song System Neurons Born during Vocal Learning in Songbirds

BENJAMIN B. SCOTT AND CARLOS LOIS*
Department of Brain and Cognitive Sciences, Picower Institute for Learning and Memory, MIT, Cambridge, Massachusetts 02139

ABSTRACT

New neurons are added to the forebrain song control regions high vocal center (HVC) and Area X of juvenile songbirds but the identity and site of origin of these cells have not been fully characterized. We used oncoretroviral vectors to genetically label neuronal progenitors in different regions of the zebra finch lateral ventricle. A region corresponding to the mammalian medial and lateral ganglionic eminences generated medium spiny neurons found in Area X and in the striatum surrounding Area X, and at least two classes of interneurons found in HVC. In addition, our experiments indicate that the HVC projection neurons that project into nucleus robust nucleus of the arcopallium (RA) are born locally from the ventricular region immediately dorsal to HVC. The ability to genetically target neuron subpopulations that give rise to different song system cell types provides a tool for specific genetic manipulations of these cell types. In addition, our results suggest striking similarities between neurogenesis in the embryonic mammalian brain and in the brain of the juvenile songbird and provide further evidence for the existence of conserved cell types in the forebrain for birds and mammals. J. Comp. Neurol. 502:202–214, 2007.
© 2007 Wiley-Liss, Inc.

Indexing terms: neurogenesis; basal ganglia; medium spiny neuron; interneuron; critical period; zebra finch

The songbird brain contains a neural pathway specialized for the production of learned vocalizations (Nottebohm, 1999). This pathway, termed the song system, consists of interconnected song nuclei located in the forebrain, midbrain, and hindbrain dedicated to processing auditory and motor signals related to song. The song system is not fully formed during the embryonic stage. Instead, it undergoes dramatic anatomical development while juvenile songbirds learn their song. During the song learning period, two song nuclei of the juvenile male songbird forebrain, the high vocal center of the nidopallium (HVC) and Area X of the striatum, greatly increase in neuron number (Nordeen and Nordeen, 1988, 1990; Alvarez-Buylla et al., 1988a). New neurons are also added to these two nuclei in adulthood, particularly at the time when the song is modified. The temporal relationship between new neuron addition and song learning has lead to the hypothesis that postnatal neurogenesis plays an important role in song learning (Alvarez-Buylla et al., 1990a; Nottebohm, 2002; Wilbrecht et al., 2006). However, the identity of the neurons added to the song system after hatching has been only partially characterized (Alvarez-Buylla et al., 1990a; Kirn et al., 1991; Sohrabji et al., 1993; Nordeen and Nordeen, 1988; Nottebohm, 2004) and detailed knowledge about their morphology, electrophysiology, and connectivity is needed to formulate realistic hypotheses about the function of postnatal neurogenesis in the songbird brain.

Telencephalic neural progenitors are known to reside in the ventricular zone (VZ) in the walls of the lateral ventricles during vertebrate embryonic development. Different subregions of the VZ are specialized for the production of different classes of neurons. The VZ of the lateral ventricle can be divided during the embryonic stage into two

Grant sponsor: Ellison Foundation.

*Correspondence to: Carlos Lois, Department of Brain and Cognitive Sciences, Picower Institute for Learning and Memory, MIT, 77 Massachusetts Ave., Cambridge, MA 02139. E-mail: los@mit.edu

Received 23 August 2006; Revised 26 October 2006; Accepted 28 December 2006

DOI 10.1002/cne.21296

Published online in Wiley InterScience (www.interscience.wiley.com).

© 2007 WILEY-LISS, INC.

WILEY InterScience

regions, the pallial VZ and subpallial VZ, each specialized for the production of different classes of neurons. The pallial VZ, which lies adjacent to the pallial anlage, expresses the T-box transcription factor TBR1 and, in mice, generates excitatory neurons of the cortex (Hevner et al., 2006). The subpallial VZ, which is adjacent to the striatal anlage, expresses the homeobox gene DLX2, and in mice gives rise to inhibitory interneurons in the striatum and cortex as well as the medium spiny neurons (MSNs) of the striatum (Marin and Rubenstein, 2003). In mammals the VZ is a transient structure that exists during a brief period during embryogenesis. In birds the VZ persists after birth (Alvarez-Buylla et al., 1998) and is thought to continue to produce new neurons into adulthood (Goldman and Nottebohm, 1983; Alvarez-Buylla and Nottebohm, 1988; Alvarez-Buylla et al., 1990a; Dewulf and Bottjer, 2005); however, the different cell types produced by the VZ after hatching remain unknown.

We sought to characterize the postnatal VZ of juvenile zebra finches and to determine the developmental origin and identity of the new neurons added to the song system. We performed immunohistochemical analysis of TBR1 and DLX expression to identify the pallial and subpallial VZ. We then used local injections of an oncoretroviral vector carrying the gene for the green fluorescent protein (GFP) to label neuronal progenitors in subregions of the VZ expressing either TBR1 or DLX genes. Thirty-five days after infection of the lateral ventricle we observed mature, GFP-positive (GFP+) neurons in HVC and Area X. Neurons in HVC that extended axons into the robust nucleus of the arcopallium (RA) appeared following the infection of the TBR1-positive (TBR1+) VZ overlying HVC. After infection of the DLX-positive (DLX+) VZ adjacent to the striatum, a region homologous to the mammalian medial ganglionic eminence (MGE) and lateral ganglionic eminence (LGE) (Puelles et al., 2000), medium spiny neurons were detected in Area X and two types of GABAergic neurons were detected in HVC.

These observations have allowed us to characterize the phenotype of the new neurons that are added into juvenile brain nuclei of the song system during the period of song learning. In addition, the identification of the site of origin of these different neuron types provides us with a convenient method to genetically manipulate the activity of song system cells. Finally, our observations reveal striking homologies between brain development in embryonic mammals and juvenile songbirds, and suggests that the array of cell types in the avian and mammalian forebrain is more similar than previously thought.

MATERIALS AND METHODS

Viral vectors

Oncoretroviral vectors based on the Moloney Murine Leukemia Virus were engineered to carry GFP under control of the internal promoter of the Rous Sarcoma Virus (Yamamoto et al., 1980), which we determined to be a strong ubiquitous promoter in zebra finch cells. Viral vectors were pseudotyped with the VSVg envelope, produced as described for lentiviruses (Lois et al., 2002) and concentrated to 10^6 infectious units (I.U.)/μL. Following concentration, vector solutions were aliquoted and stored at −80°C.

Surgery

Zebra finches were obtained from our breeding colony at MIT. Twelve males were injected bilaterally into either the subpallial or pallial VZs 28–48 days after hatching. Bilateral injections were also made into the pallial VZs of four adult females. Stereotaxic coordinates used were based on the expression of marker proteins TBR1 and the DLX family and initially determined using stereotaxic coordinates derived from the canary atlas of Stokes et al. (1974) and subsequently confirmed empirically. The head of the bird was placed in a stereotaxic head holder at an angle of 45° and we defined the branch point of the sagittal sinus that lies just anterior to the rostral tip of the cerebellum as stereotaxic point 0.0 both for the anteroposterior and the mediolateral axes. To target the subpallial VZ we used the following coordinates: 1.6 mm anterior, 4.4–4.8 mm lateral, 3.75–3.85 mm bellow the dura and an injection angle tilted 45° relative to the horizontal plane. To target the VZ just dorsal to HVC we penetrated the brain perpendicular to the surface of the brain (90° vertical injection angle relative to the horizontal plane) and used the following coordinates: 0.3 mm anterior, 2.2 mm lateral, 0.17–0.3 mm deep.

Injection needles were constructed from pulled borosilicate capillary tubes (Sutter Instrument, Novato, CA) with a fine taper, whose tip had been cut to 20–50 μm inner diameter using a ceramic cutting tile (Sutter Instrument). Then 100–1,000 nL of vector solution was delivered by slow (0.5 nL per second) injection using a micropump (WPI, Sarasota, FL). Following surgery, animals were returned to our colony where they were housed with their family (if younger than 40 days posthatch) or other juvenile males (if older than 40 days posthatch).

For retrograde tracing of HVC_{RA} projection cells, we injected 30 nL of FluoroGold (Fluorochrome, Englewood, CO) in the right RA and 30 nL of cholera toxin subunit B conjugated to Alexa Fluor 555 (Molecular Probes, Eugene, OR) in the left RA. FluoroGold was used as a tracer to allow comparison with previous studies that used this tracer. Cholera toxin subunit B conjugated to Alexa Fluor 555 was used to allow visualization of these cells by confocal microscopy. These injections were performed 7 days prior to perfusion. One juvenile zebra finch became ill 4 days after the RA injections and was perfused immediately. Previous studies have shown that 4 days are sufficient for retrograde tracing and we noticed no difference in the percentage of GFP+ cells retrogradely labeled in this animal or in the morphology of GFP+ cells.

Histology and immunohistochemistry

Juvenile zebra finch males were deeply anesthetized with ketamine and xylazine and perfused intracardially with 20 mL of phosphate-buffered saline (PBS), pH 7.4, followed by 3% paraformaldehyde in PBS (50 mL). Brains were removed from the skull and soaked in 3% paraformaldehyde for 12–24 hours at 4°C. After fixation, brains were washed with PBS and cut to 30, 50, or 100 μm sections with a vibrating microtome (Leica, Deerfield, IL).

Immunohistochemistry was performed with the following antibodies: NeuN was detected using a mouse monoclonal antibody (diluted in blocking solution 1:500) (Chemicon, Temecula, CA; MAB377, lot 19060600) raised against purified cell nuclei from the mouse brain. According to the manufacturer this antibody stains 2–3 bands in

the 46–48 kD range and 0–1 bands of molecular weight 66 kD on Western blot. Immunohistochemistry against NeuN is widely used to stain neurons; however, the identity of the antigen is not known. We used anti-NeuN to identify the borders of the song nuclei HVC and Area X. GABA was detected using a rabbit polyclonal antibody (diluted 1:2,000) (Sigma, St. Louis, MO; A2052, lot 095K4830) raised against GABA-BSA. According to the manufacturer this antibody shows positive binding to GABA and negative binding to BSA in a dot blot assay. Parvalbumin was detected using a mouse monoclonal antibody (diluted 1:1,000) (Sigma, P3088, lot 075K4794) raised against purified frog muscle parvalbumin. According to the manufacturer this antibody stains a 12-kD band on Western blot. DARPP-32 was detected using a mouse monoclonal antibody (diluted 1:10,000; clone C24-5a), a gift of H.C. Hemmings (Cornell University), raised against purified bovine DARPP-32. This antibody stains a single band of molecular weight 32 kD on Western blot (Hemmings and Greengard, 1986). A rabbit polyclonal antibody (diluted 1:1,000) against DLX family members was used to identify the subpallial portion of the juvenile zebra finch VZ. The antibody, a gift of S.B. Carroll (University of Wisconsin), was raised against a synthetic peptide corresponding to the following 61-amino acid homeodomain of butterfly DLL: MRKPRTIYSSLQLQQLNRRFQRTQYLALPERAE-LAASLGLTQTQVKIWFQNRRSKYKKMMK. This antibody recognizes a conserved homeodomain found in DLL and DLX proteins in arthropods (Panganiban et al., 1995) and vertebrates (Brown et al., 2005). TBR1 was detected using a rabbit polyclonal antibody (diluted 1:100), a gift of M. Sheng (MIT), raised against a synthetic peptide corresponding to residues 614–624 of mouse TBR-1 (Hsueh et al., 2000). This antibody has been shown to stain a band of molecular weight 85 kD in Western blots from mice and rat brains (Wang et al., 2004). The monoclonal antibody 39.4D5 (diluted 1:500), obtained from the Developmental Studies Hybridoma Bank (Iowa City, Iowa), was used to detect the region of the VZ putatively homologous to the mammalian lateral ganglionic eminence. This antibody was raised against a synthetic peptide corresponding to amino acid residues 178–349 of rat ISL-1 and has been shown to stain both ISL-1- and ISL-2-positive cells (Tsuchida et al., 1994) and has previously been used to identify the lateral ganglionic eminence in mice (Stenman et al., 2003). A monoclonal antibody against Nkx2.1 (Labvision, Fremont, CA; clone 8G7G3/1 lot 699p212) (diluted 1:100) was used to detect the region of the VZ putatively homologous to the mammalian medial ganglionic eminence. According to the manufacturer, this antibody was raised against rat TTF-1 (NKX2.1) and stains a band of molecular weight 40 kD on Western blots.

Tissue sections were placed in blocking solution containing 10% normal goat serum (Hyclone, Logan, UT), 0.25% Triton X-100 (Sigma) in PBS for 20 minutes. Tissue sections were then incubated in antibody diluted in blocking solution for 1 hour, washed 3 times in PBS, and incubated in secondary antibody for 1 hour. Alexa Fluor 555 conjugated goat antimouse (Molecular Probes) and Alexa Fluor 488 conjugated goat antirabbit (Molecular Probes) secondary antibodies were used diluted to 1:250 in blocking solution. Cy5 antirabbit (Jackson Laboratories, West Grove, PA) was used diluted to 1:100 in blocking solution.

Colabeling of antibodies and GFP was determined using confocal microscopy. In many cases antibodies could not penetrate deep enough into the tissue section to reach the depth of the cell bodies of GFP+ neurons. In these cases, since we were unable to determine whether the neuron expressed the particular antigen, we did not include those GFP+ cells in our immunohistochemical analysis.

Image acquisition and processing

Photomicrographs were obtained using a Nikon PCM2000 confocal microscope or an Olympus IX70 epifluorescence microscope and Retiga 1300 digital CCD camera (Qimaging, Surrey, BC, Canada). Neurolucida (MicroBrightField, Williston, VT) was used to trace and record the positions of new neurons and song nuclei from brain sections. Photoshop (Adobe Systems, Mountain View, CA) was used to add color, merge images, and adjust contrast and brightness. ImageJ was used to merge serial sections acquired with the confocal microscope.

RESULTS

Expression patterns of homeobox and T-box transcription factors in the ventricular zone of juvenile songbirds

To determine whether the VZs of juvenile songbirds and embryonic birds and mammals maintain similar patterns of gene expression, we examined the expression of TBR1 and members of the DLX gene family using antibodies raised against the C-terminus of TBR1 (Hsueh et al., 2000) and against a protein domain that is conserved among members of the DLX gene family (Panganiban et al., 1995). DLX-positive (DLX+) cells were present in the ventral VZ ranging from the ventral end of the ventricular wall to the border of the mesopallium–nidopallium (Fig. 1D). The highest level of expression was observed in the ventricular wall adjacent to the striatum. This region corresponds to the previously described ventral proliferative "hot spot" that contains a high number of mitotic cells and radial glia (Fig. 1C) (Alvarez-Buylla et al., 1990b; Dewulf and Bottjer, 2005). DLX+ cells were also observed in the striatum itself, in the medial pallium, and to a lesser extent in the lateral and dorsal pallium.

In the mammalian embryo the DLX-expressing region of the VZ is further divided into the LGE and the MGE. A region homologous to the mammalian LGE and MGE has also been previously described in embryonic chick brain (Puelles et al., 2000). In mice the LGE can be detected using antibodies against homeodomain-containing transcription factors ISL-1 and ISL-2 (ISL-1/2) (Stenman et al., 2003). This region is believed to be the source of the medium spiny neurons of the striatum (Deacon et al., 1994; Wichterle et al., 2001). The MGE can be identified by expression of the homeodomain-containing transcription factor NKX2.1 and is thought to be the source of cortical parvalbumin- and somatostatin-expressing interneurons (Xu et al., 2004) (Butt et al., 2005). In the DLX+ portion of the lateral ventricle in the juvenile zebra finch we observed expression of both ISL-1/2 and NKX2.1 (Fig. 1F,G), suggesting the existence of LGE-like and MGE-like progenitor zones in the postnatal songbird brain. ISL-1/2 was expressed throughout the VZ adjacent to the striatum and NKX2.1 was expressed primarily in the ventralmost portion of the lateral ventricle.

TBR1 was expressed throughout the lateral and dorsal pallium and in the adjacent VZ (Fig. 1E). The density of

TBR1 cells was highest in the hyperpallium and mesopallium, lower in the nidopallium, and lower still in the arcopallium. TBR1 expression was absent from the striatum, thalamus, hippocampus, and cerebellum. Interestingly, HVC and RA contained a higher density of cells and a greater intensity of TBR1 staining than surrounding brain regions. Cells in the lateral magnocellular nucleus of the nidopallium (LMAN) were also positive for TBR1, although the cell density and signal intensity were not obviously different from the surrounding nidopallium.

Expression of TBR1 was highest in HVC, the wall of the lateral ventricle dorsal to HVC (data not shown), and in the anterior edge of the dorsal aspect of the lateral ventricle. This latter region is rich in radial glia and corresponds anatomically to the dorsal proliferative "hot spot" previously described (Alvarez-Buylla et al., 1990b; Dewulf and Bottjer, 2005). Although the VZ dorsal to HVC contains vimentin-positive cell bodies, few vimentin-positive fibers enter HVC (Alvarez-Buylla et al., 1988b). Long-distance migration of precursors for projection neurons is thought to depend on guidance provided by the long processes of radial glia. The scarcity of vimentin-positive radial fibers through HVC suggests that neurons born in the VZ dorsal to HVC may not have the ability to distribute throughout the pallium and might instead migrate exclusively into HVC.

Fate of the cells derived from the pallial ventricular zone above HVC

Based on the pattern of TBR1 expression in the finch forebrain that we observed, we hypothesized that HVC to RA projection neurons (HVC_{RA}) might originate in the dorsal portion of the VZ. The presence of vimentin-positive cells and many TBR1+ cells contained in the VZ immediately dorsal to HVC supported a hypothesis by Goldman and Nottebohm (1983) that this region of the lateral ventricle in particular might produce HVC_{RA} neurons. To test this hypothesis we used an oncoretroviral vector carrying the gene for GFP to follow the fate of neuronal progenitors in three different regions of the VZ of three juvenile zebra finches (age 28–48 days) and in four different regions in four adult female (age 90–94 days) zebra finches that spanned the TBR1+ portion of the lateral ventricle. Viral vectors based on oncoretroviruses readily infect mitotically active cells but are unable to infect nondividing cells (Roe et al., 1993) such as neurons. Animals were sacrificed 35 days after virus injection and their brains prepared for

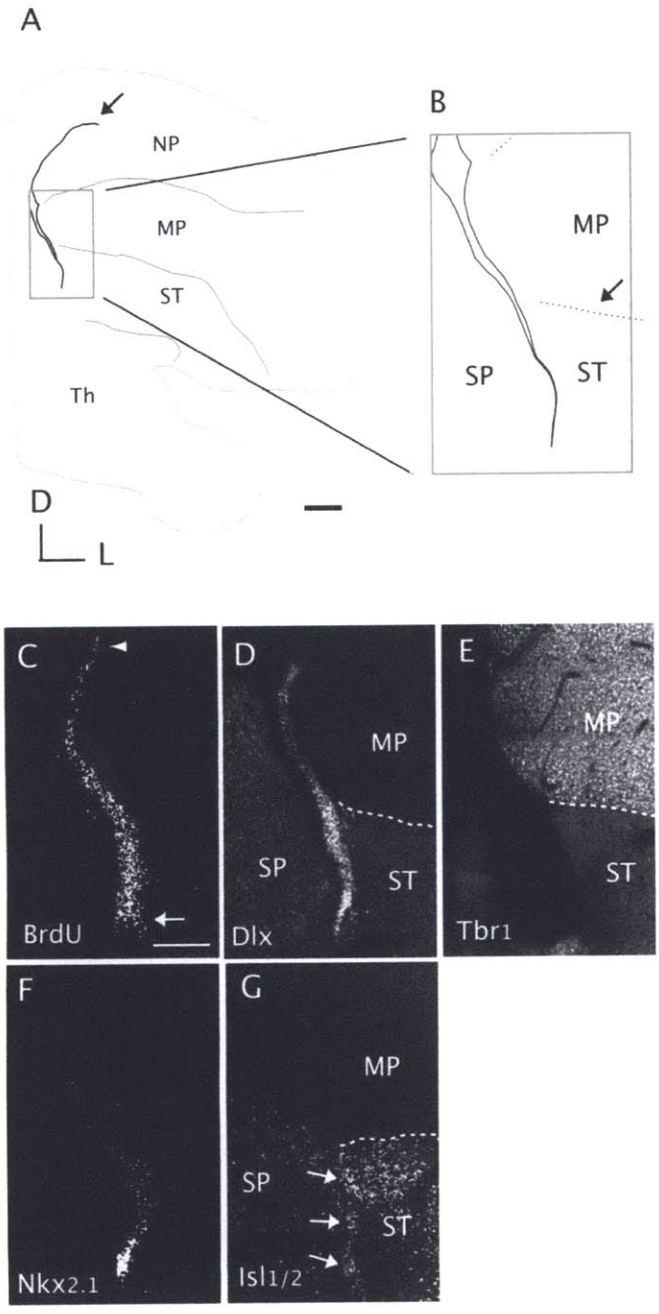

Fig. 1. Expression of homeobox and T-box transcription factors in and near the lateral ventricle of the juvenile zebra finch. **A:** Schematic diagram of the left hemisphere of the finch brain in a frontal section at the level of the anterior commissure, roughly 3.0 mm anterior of bregma. The dark line (arrow) identifies the lateral ventricle. Thin solid lines indicate the laminar divisions of the forebrain. NP, nidopallium; MP, mesopallium; ST, striatum; Th, thalamus. The box identifies the region of the lateral ventricle shown in B–E. **B:** Diagram of the region pictured in C–F. The solid black line indicates the lateral ventricle. The dotted line (arrow) represents the laminar division that separates the mesopallium (MP) from the striatum (ST). The septum (SP) lies medial to the lateral ventricle. **C:** BrdU staining in the wall of the lower region of the lateral ventricle. The highest level of cell proliferation was observed in the VZ from the border of the mesopallium (arrowhead) to the ventral tip of the lateral ventricle (arrow). This region corresponds to the ventral proliferative "hot spot" described before (Alvarez-Buylla et al., 1990b). **D:** DLX expression in the lateral ventricle and surrounding brain regions. Expression of DLX is highest in the BrdU-positive region of the lower part of the lateral ventricle. However, DLX staining was also observed in the striatum (ST), the septum (SP), and to a lesser extent in the pallium (MP). The dotted line indicates the pallial–striatal border. **E:** TBR1 is expressed exclusively in the pallium and pallial ventricular zone. The TBR1+ zone abruptly stopped at the pallial–striatal border (dotted line). **F:** Expression of NKX2.1 was primarily restricted to the ventralmost portion of the lateral ventricle. The pattern of NKX2.1 expression also overlapped with the expression of pattern of ISL-1/2, suggesting that in the juvenile finch brain the LGE-like region and MGE-like region are not completely segregated. **G:** Expression of ISL-1/2 in and around the lateral ventricle. ISL-1/2 was observed in the striatum (ST), the septum (SP), and in the lowest part of the VZ adjacent to the striatum (arrows). Dotted line indicates the pallial–striatal boarder. Scale bars = 1 mm in A; 0.5 mm in C (applies to D–G).

histological analysis. All seven injection sites produced many (>25) GFP+ cells with similar appearance that were found in long clusters that extended ≈200–800 μm along an axis perpendicular to the VZ at the injection site. All had round cell bodies and thin, spiny dendrites. Of these different locations, only injections into the lateral ventricle directly dorsal to HVC produced GFP+ cells in HVC. Once we determined that the VZ dorsal to HVC was a source for HVC cells, we injected three juvenile males 28–35 days posthatch with our oncoretroviral vector in this region. To confirm the identity of HVC_{RA} projection neurons, small injections of a retrograde tracer (Fluoro-Gold or cholera toxin conjugated to Alexa Fluor 555) were made into RA 4 or 7 days prior to perfusion (see Materials and Methods).

To determine the spread of infection and to identify cell types infected by our oncoretroviral vector we injected an additional three birds (males age 28–48 days posthatch) in the ventricular zone dorsal to HVC and examined the distribution of GFP-labeled cells 2–4 days later. Two days after infection GFP+ cells were observed within the VZ near the injection site and in the surrounding brain region (data not shown). Most GFP+ cells were observed within 300 μm of the injection site, and no cells were observed further than 600 μm from the injection site. These cells had round cell bodies and many appeared to have short processes oriented parallel to the ventricular wall. We inferred that these cells had undergone recent mitosis but had not yet acquired a phenotype that identified what kind of cell they would become.

Four days after infection GFP+ cells were observed in the VZ and nidopallium at distances up to 600 μm away from the injection site (Fig. 2A). At this time many cells had a morphology characteristic of migratory neurons, with a long leading process that terminated in a growth cone, a small round cell body, and a short trailing process. Interestingly, no cells with radial glia-like morphology were observed at any survival time. In addition, we never observed cells remaining in the VZ after long survival times (35 days).

Five weeks after injections targeted to the VZ above HVC, GFP+ neurons were observed in HVC and the nidopallium adjacent to HVC (Fig. 3A,B). Interestingly, no GFP+ cells remained in the VZ, nor did any GFP+ cells appear to be in the process of migration. All GFP+ cells inside HVC had a similar morphology (Fig. 3C,D). These cells had small round cell bodies between 7 and 12 μm in diameter (mean, 10.0 μm; n = 28), and thin spiny dendrites that appeared to be confined to HVC. Many GFP+ axons were visible and could be seen to exit the posterior border of HVC, project along the posterior region of the nidopallium, and enter RA, where they branched extensively. Most axons wandered in and out of the 100-μm sections. However, in one case we were able to observe an axon in its entirety projecting from HVC to RA in the same section (Fig. 4A). We observed at least two general pathways of entry into RA (Fig. 4B,C). Some axons appeared to enter RA at its most posterior aspect and branch as they entered the nucleus. Other axons appeared to arrive at the dorsal border of RA, then turn anterior and skirt the dorsal edge of the nucleus, and finally enter RA further toward its anterior tip. Interestingly, some cells appeared to bundle their axons together over the course of their projection (Fig. 4D). Even though retrograde injections covered the extent of RA, only about half (18/32) of the

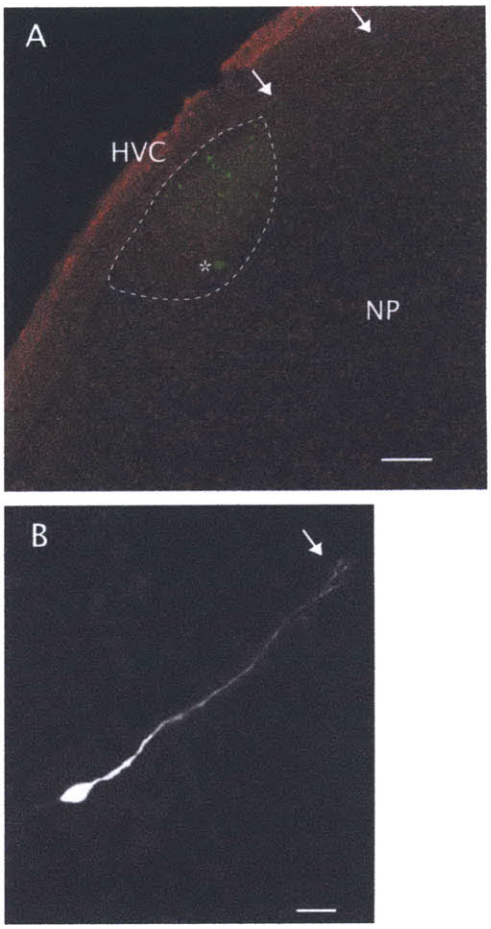

Fig. 2. Distribution of GFP+ cells shortly after injection of retrovirus into HVC. **A:** Parasagittal section of the posterior forebrain of a bird perfused 4 days after injection of oncoretroviral vector. The section is immunostained with anti-NeuN (red) to identify the borders of HVC. Dotted line indicates the border of HVC. GFP+ cells were observed along the lateral ventricle (arrows) and within HVC. Four days after infection cells were observed up to 600 μm from the injection site. The asterisk identifies a region of autofluorescence, which was an artifact of tissue processing. NP, nidopallium. **B:** Migrating GFP+ cell derived from the DLX+ region of the lateral ventricle 7 days after injection. The cell had a short trailing process, a small cell body, and a long leading process with a growth cone at its tip (arrow). This morphology is typical of GFP+ cells observed 2–7 days after infection, and similar to that of migrating cells in the adult avian and embryonic mammalian brain. This cell was found in the wall of the lateral ventricle dorsal to the injection site with its leading process oriented dorsally toward the pallium. Scale bars = 200 μm in A; 10 μm in B.

GFP+ neurons in HVC were labeled with retrograde tracer. Previous studies have obtained similar percentages of BrdU+ cells backfilled from RA 30 days after BrdU injection, and have noted that the percentage of colabeled cells increases over time (Kirn et al., 1991, 1999). This suggests that at least a portion of our GFP+ cells in HVC that were not backfilled were somewhat immature HVC_{RA} neurons. Moreover, all GFP+ cells appeared similar in appearance to previously described HVC_{RA} cells (Mooney and Prather, 2005). These observations suggest the following, not necessarily mutually exclusive, possibilities: 1) In addition to HVC_{RA} cells, the VZ above HVC produces a

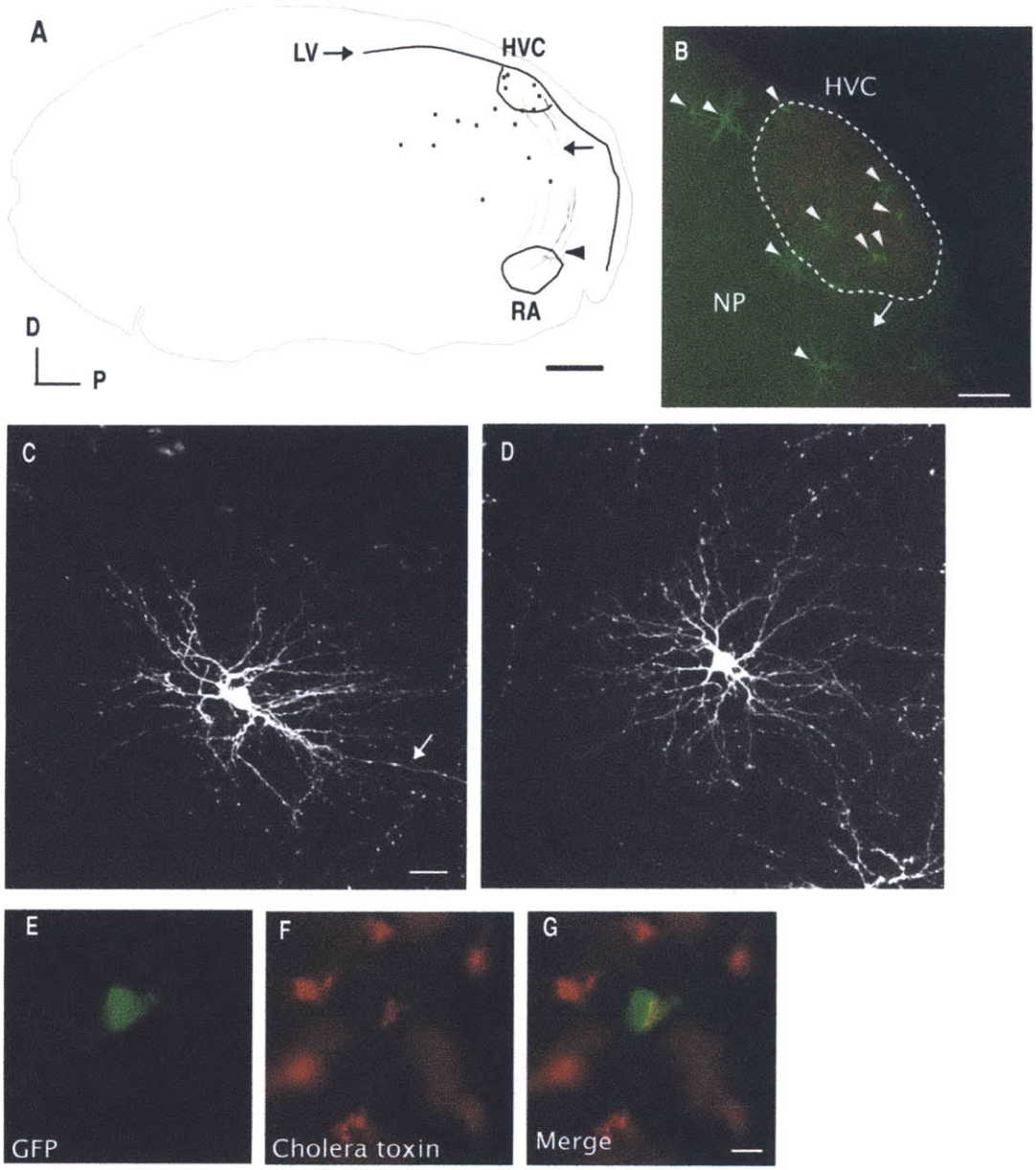

Fig. 3. Addition of new projection cells to HVC during song learning. **A:** Tracing of a parasagittal forebrain section obtained from a posthatch day 65 zebra finch 35 days after injection in the VZ dorsal to HVC. Cells (black squares) were observed in HVC and the surrounding nidopallium. Thick black lines indicate the lateral ventricle (LV) and the boundaries of HVC and RA. Axons were observed originating from HVC (arrow) and entering RA (arrowhead). **B:** GFP+ neurons (green, indicated by arrowheads) were observed in HVC and the surrounding nidopallium (NP). HVC to RA projecting neurons are labeled with a retrograde tracer injected into RA (red). GFP positive axons (arrow) can be observed exiting the posterior portion of HVC. **C:** Image of a GFP+ cell within HVC. The morphology of this cell is typical of the HVC cells that project to RA, with small round body, thin spiny dendrites, and a prominent axon (arrow). **D:** Image of a second GFP+ cell within HVC for comparison. **E–G:** GFP+ cells in HVC labeled with the retrograde tracer cholera toxin injected into RA. E: GFP+ cell. F: Alexa Fluor 555 conjugated to cholera toxin. G: Merged images of GFP and Alexa Fluor 555 conjugated to cholera toxin. Scale bars = 1 mm in A; 100 μm in B; 20 μm in C (applies to D); 10 μm in G (applies to E,F).

class of spiny interneurons that do not project to RA. 2) Some HVC_{RA} neurons had not yet extended axons into RA 35 days after their birth. 3) Labeling of HVC_{RA} cells with certain retrograde tracers may be partial, so that only a portion of cells with axons within RA are backfilled. Some GFP+ neurons were observed in the nidopallium outside HVC. These cells were morphologically similar to HVC_{RA} cells but, in general, had thicker dendrites that were more densely covered with spines. In addition, their axons were thin and difficult to detect and we did not characterize their projection pattern.

Fate of cells derived from the ventricular zone adjacent to the striatum

To follow the fate of cells born in the DLX+ portion of the lateral ventricle adjacent to the striatum, we injected

this area with 150–1,000 nL of oncoretroviral vector and 35 days after infection we examined the identity and position of the GFP+ cells. Although we did not attempt to thoroughly characterize the migration patterns of these cells, we examined one bird 7 days after infection. We observed cells that, based on their morphology, appeared to be in the process of migration in two directions, 1) dorsally toward the pallium along the wall of the lateral ventricle, and 2) laterally along the radial glia tracts that run in the lamina that separates the striatum and pallium. These cells had a long leading process, whose orientation we used to infer direction of migration, with an apparent growth cone at its distal end, and a short presumed trailing process (Fig. 2B). These cells resembled migrating neuroblasts in the developing mammalian cortex. Cell migration from the subpallial VZ into the pallium has been observed before in embryonic birds and mammals (Cobos et al., 2001; Marin and Rubenstein, 2003), and is thought to take place by a distinct type of migration, called tangential migration, that occurs independent of radial glia. Five weeks after infection, no migrating GFP+ cells remained; instead, all labeled cells appeared to have a mature neuronal phenotype. Mature GFP+ cells appeared distributed throughout the hyperpallium, mesopallium, nidopallium (including HVC), and striatum (including Area X) (Fig. 5A). The furthest cell appeared more than 8 mm away from the site of injection. Few GFP+ cells were detected in the arcopallium, a brain region that has been shown to have a low rate of new neuron incorporation after hatching (Alvarez-Buylla et al., 1994).

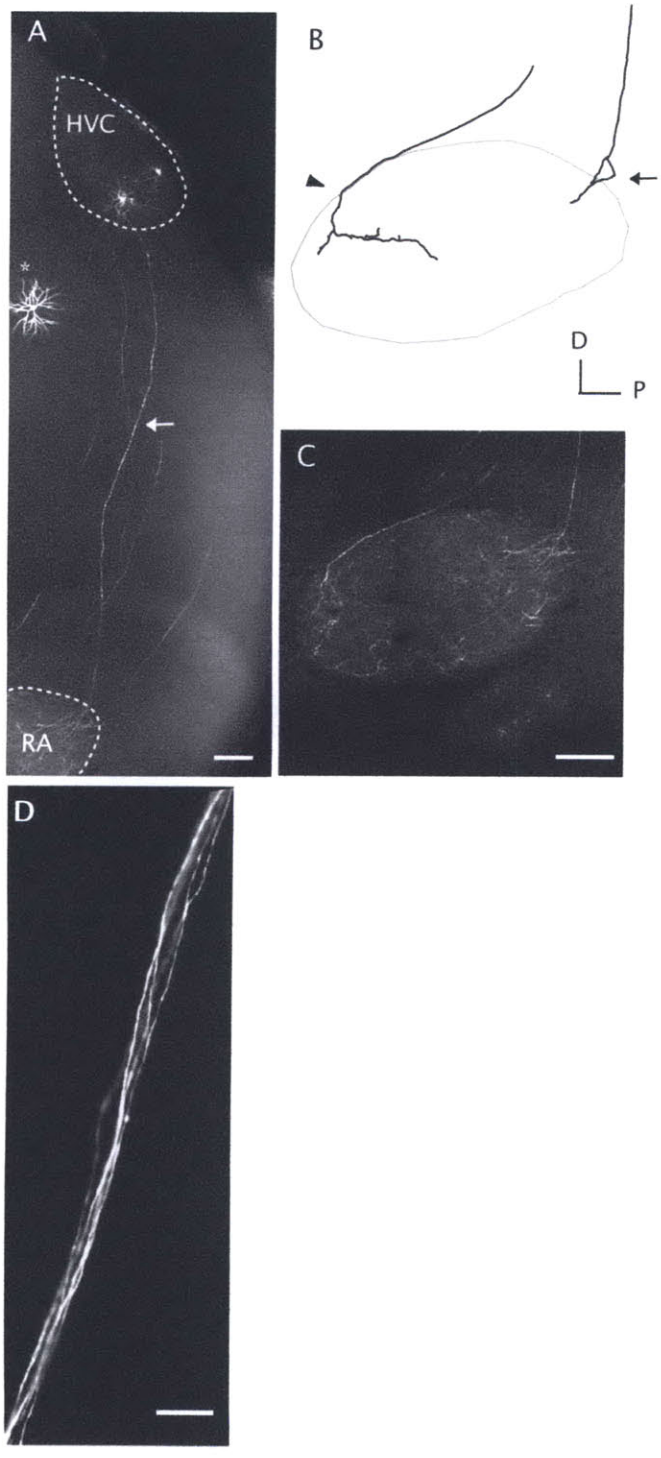

Area X. The vast majority of the GFP+ cells in the striatum had a morphology that was distinct from the cells observed in HVC. Labeled cells in Area X had highly branched dendritic arbors and an axon that appeared confined to Area X. The soma of GFP-labeled cells in Area X was between 6 and 10 μm in diameter (mean, 7.7 μm; n = 49), and their dendrites were densely covered with spines (Fig. 5C–E). These cells bore close resemblance to the previously characterized spiny neurons of Area X (Farries and Perkel, 2002) and to the medium spiny neurons of the mammalian striatum (Wilson, 2004). To further characterize this cell population we performed immunohistochemistry against DARPP-32 (Fig. 5F–H), a specific marker for medium spiny neurons in the mammalian and avian striatum (Anderson and Reiner, 1991; Reiner et al., 1998). The DARPP-32 antibody did not penetrate deeply into our vibratome sections and therefore we were only able to characterize seven GFP+ cells in the superficial region of our sections. Six of these seven cells were also positive for DARPP-32.

HVC. GFP+ cells were also detected throughout the pallium including HVC and HVC shelf (Figs. 6D, 7D). The number of new neurons that were detected in HVC after viral injection in the lower region of the VZ was relatively low (16 neurons from four injected hemispheres). It is important to notice that HVC occupies only a very small percentage of the volume of the forebrain and perhaps,

Fig. 4. Characterization of HVC projection cells born during vocal learning. **A:** GFP-labeled cells in HVC and the surrounding nidopallium following infection of the VZ dorsal to HVC. GFP+ axon (arrow) from HVC to RA observed in its entirety. A GFP-labeled cell outside of HVC is labeled with an asterisk. **B:** Tracing of the innervation of RA by axons of HVC projection cells. Two patterns of innervation were observed. Some axons, such as the one pictured in A, entered RA at the posterior end of the nucleus (arrow). Other axons appeared to skirt the dorsal edge of RA and enter the nucleus at the anterior edge (arrowhead). In either case the axon of the HVC projection cell ramified immediately upon entry into RA sending out at least two collaterals that branched extensively throughout the nucleus. **C:** Photograph of the innervation of RA used to produce the tracing in B. **D:** Axon bundles in the HVC to RA projection. Scale bars = 250 μm in A; 200 μm in C; 10 μm in D.

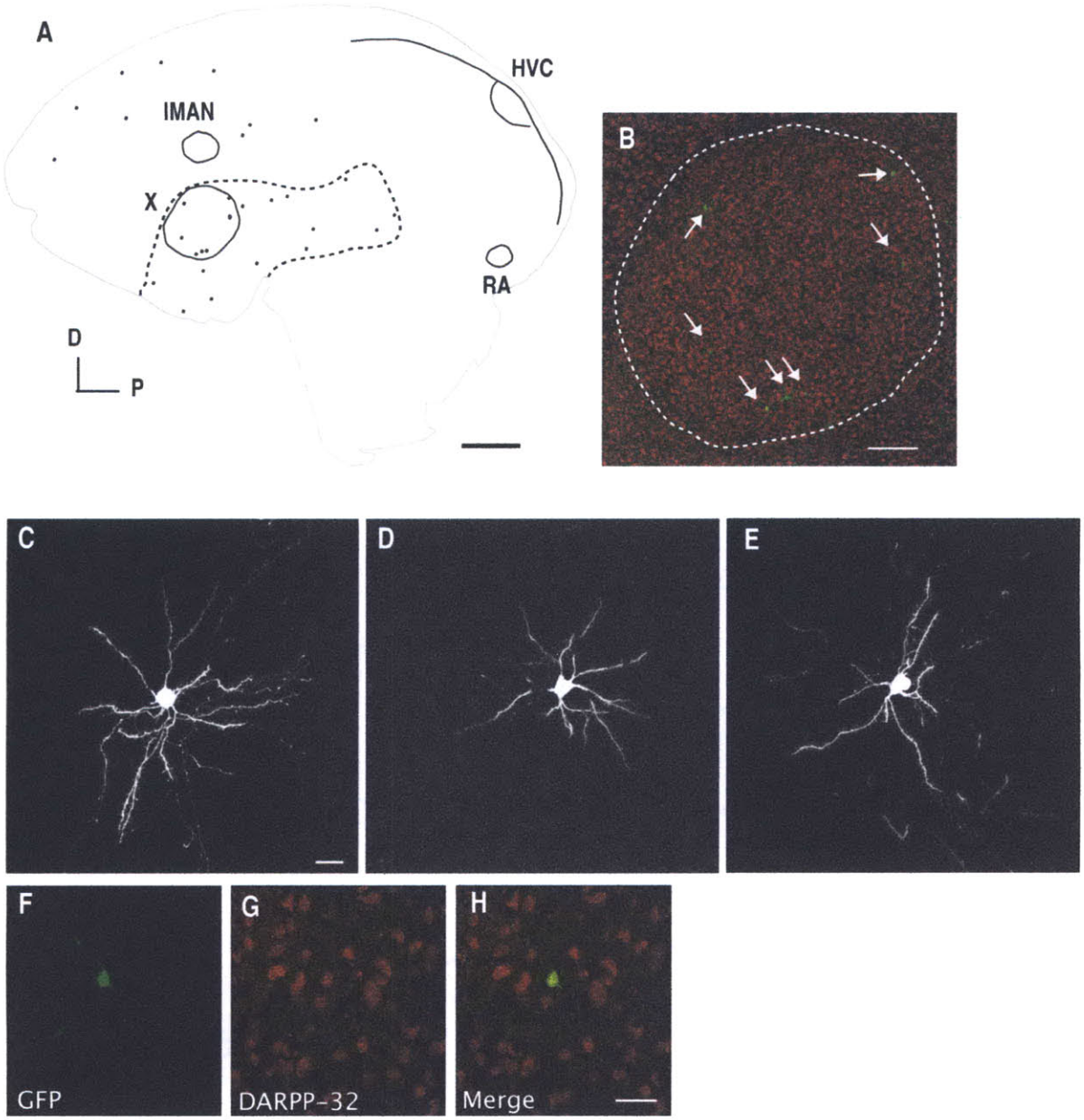

Fig. 5. Neuron addition in Area X. **A:** Tracing of the distribution of GFP+ cells in a parasagittal section of the zebra finch forebrain 35 days after infection of the ventral VZ with retroviruses. Cells (black squares) could be observed throughout the striatum, including Area X and pallium (dotted line indicates the border of the striatum and pallium). New neurons were also detected in HVC, although not in this section. **B:** GFP+ cells (green, indicated by arrows) in Area X immunostained with an antibody against NeuN (red). Dotted line indicated the border of Area X. **C–E:** Confocal microscopy images of GFP+ cell in Area X (C,D) and surrounding striatum (E) 35 days after infection of the avian MGE and LGE. The morphology of these cells is characteristic of GFP+ cells in Area X and the surrounding striatum. These cells had small cell bodies and thick spiny dendrites. (F-H) GFP+ cells in Area X express DARPP3-32. **F:** GFP cell body in Area X imaged with confocal microscope. **G:** DARPP-32 immunostaining in the same optical section as D. **H:** Merged images of GFP and DARPP-32 immunostaining. Scale bars = 1 mm in A; 200 μm in B; 10 μm in C (applies to D,E); 25 μm in H (applies to F,G).

accordingly, it may only receive a small percentage of the neurons produced in this area of the VZ. In addition, the low number of GFP+ cells observed following injection of the DLX-expressing region of the VZ could reflect a low rate of interneuron addition in HVC at the age our birds were injected. We observed at least two distinct cell morphologies in HVC and HVC shelf. The first cell type observed (9/16) had an oblong cell body of about 9 by 14 μm in size, a large dendritic tree with few primary dendrites, and an axon that appeared confined to HVC. The dendrites were thicker than those of the HVC_{RA} projection cells and they were densely covered with large spines (Fig. 6A–C). This cell type resembles previously characterized neurons in the canary HVC identified by horseradish peroxidase (HRP) filling of neurons (Paton and Nottebohm, 1984) and by Golgi stain (Nixdorf et al., 1989). Immuno-

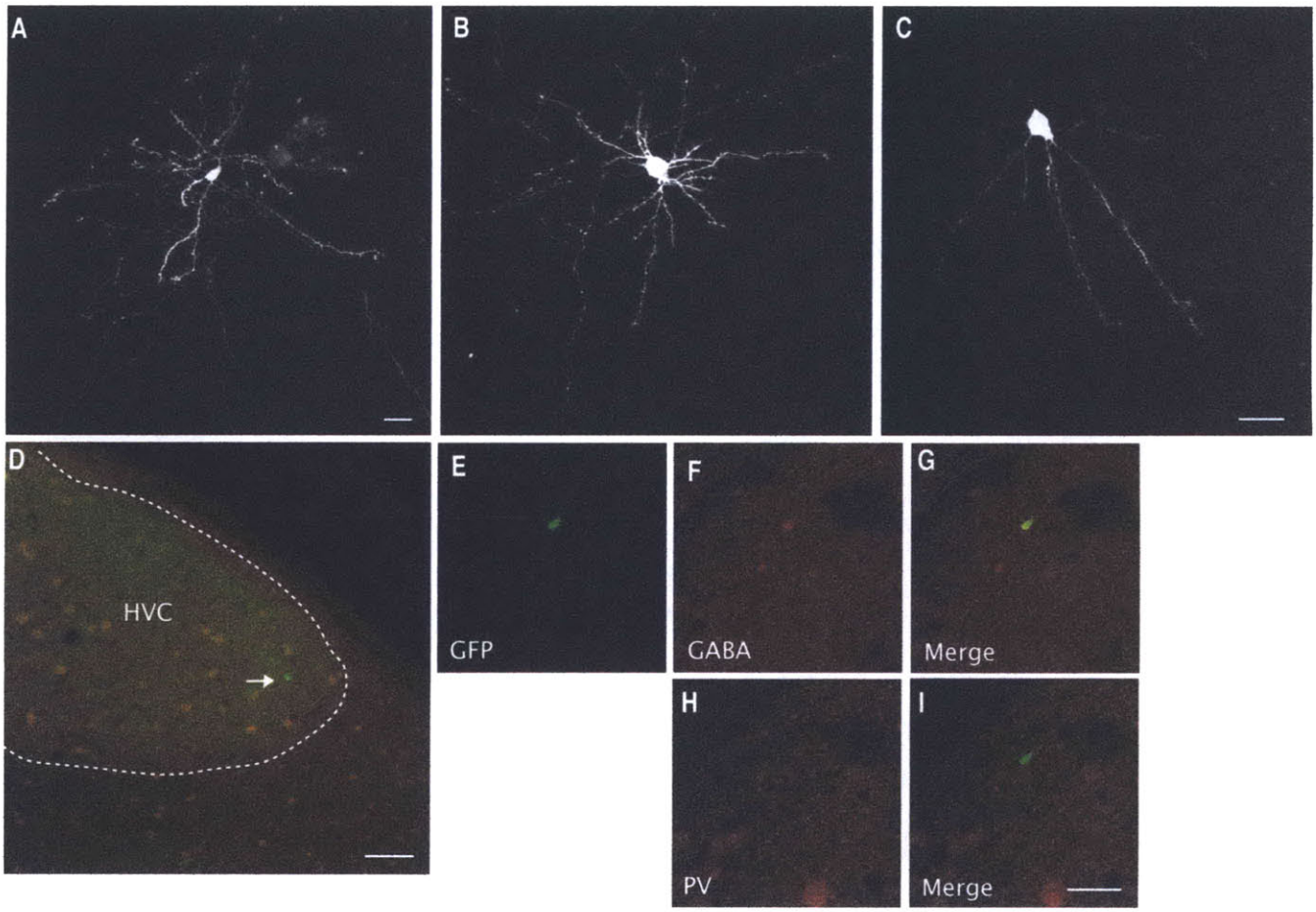

Fig. 6. Newly generated spiny interneuron in HVC. **A–C:** Three examples of new spiny interneurons in HVC born in the ventral ventricular zone. These cells were characterized by their small oblong cell bodies and thick spiny dendrites. **D:** GFP+ cell (green, indicated by arrow) observed in a parasagittal section containing HVC. Immunohistochemistry against parvalbumin (red) is used to identify the boundary of HVC. Dotted line indicates the border of HVC. **E–I:** Immunohistochemical analysis of spiny interneurons in HVC using confocal microscopy. E: GFP+ cell body in HVC. F: GABA immunostaining. G: Merged images of GFP and GABA-immunostaining. H: PV staining of the same region. I: Merged images of GFP and PV immunostaining. Scale bars = 20 μm in A,C (applies to B); 100 μm in D; 50 μm in I (applies to E–H).

staining of these GFP+ cells revealed that they were positive for GABA and negative for the calcium-binding protein parvalbumin (PV) (Fig. 6E–I). In some cases parvalbumin-positive (PV+) processes appeared to surround the cell bodies of these neurons (Fig. 7H). The pattern of parvalbumin staining appeared identical to the previously described staining pattern in HVC (Wild et al., 2005).

We observed a second neuron type in HVC and the surrounding nidopallium with large round cell bodies, between 11 and 17μm in diameter, and large dendritic arbors (Fig. 7A–C). The dendrites of these cells were either aspiny or sparsely covered with thin spines or filopodia. We observed this cell type less frequently (4/16). We were able to characterize three out of these four cells by immunohistochemistry. All three neurons were immunopositive for GABA, and two expressed PV (Fig. 7E–J). These cells were similar to the fast-spiking PV+ inhibitory neurons in the zebra finch HVC (Mooney and Prather, 2005), as well as the PV+ inhibitory basket cells found in mammalian hippocampus (Somogyi and Klausberger, 2005) and cortex (Kawaguchi and Kubota, 1996).

Three cells (3/16) could not be easily assigned to either category. By some estimates, the number of cell types in the mammalian cortex and hippocampus is extremely large (Markram et al., 2004) and often neurons are difficult to assign to a particular type (Parra et al., 1998). The cell type composition of HVC may be as diverse as the mammalian cortex, and the unassigned cell types we observed could reflect the diversity of HVC interneurons. Alternatively, our inability to assign some neurons to a particular class may be a consequence of our histological analysis. In this study, tissue sections were cut thin (30 μm) to allow better immunohistochemical analysis. For some cells (n = 2), however, the tissue sections were too thin to adequately characterize their dendritic morphology. Future experiments labeling greater numbers of HVC interneurons will be necessary to address these uncertainties about the number of different interneuron subtypes in HVC. Our method, based on fate mapping by oncoretroviral vectors, is likely to be biased for the detection of different cell types and there may be yet additional cell classes added to the song circuit during vocal learning.

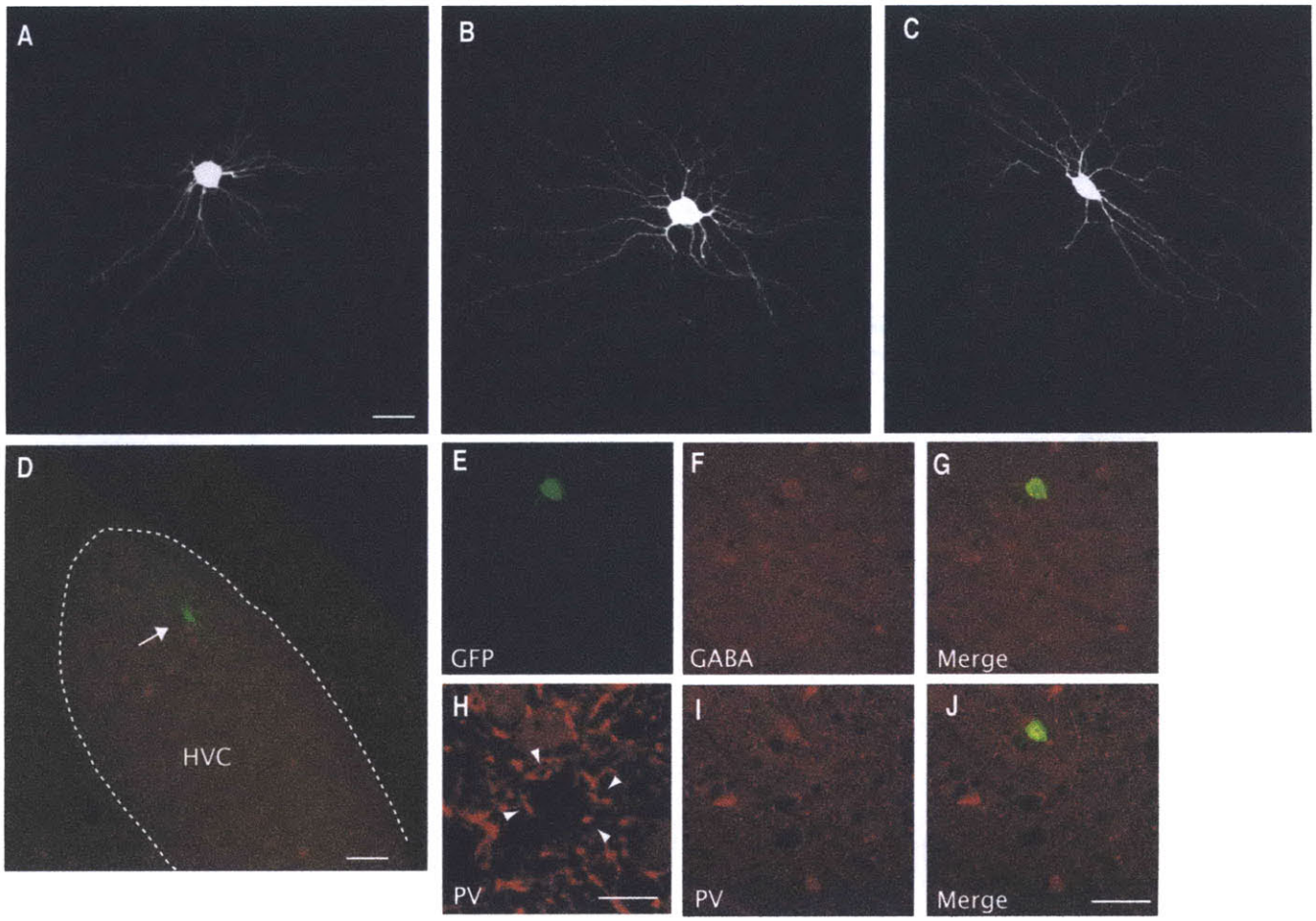

Fig. 7. Newly generated aspiny interneuron in HVC. **A–C:** Confocal microscopy images of three aspiny interneurons in HVC originating from the ventral ventricular zone. These cells were characterized by their large cell bodies and aspiny dendrites. **D:** GFP+ aspiny interneuron (arrow) in a parasagittal section of HVC. Immunohistochemistry against parvalbumin (red) is used to identify the boundary of HVC. Dotted line indicates the border of HVC. Although aspiny interneurons in HVC typically express parvalbumin, this particular cell did not. This cell is pictured at higher magnification in C. **E–J:** Immunohistochemical analysis of aspiny interneurons. E: GFP+ cell body in HVC. F: GABA immunostaining. G: Merged images of GFP and GABA-immunostaining. H: High-magnification image of parvalbumin staining. Parvalbumin was detected in cell bodies and neuropil in HVC. Parvalbumin staining revealed many varicosities (arrowheads) that often appeared to surround spherical PV− zones. These zones are probably the cell bodies of other neurons, since we sometimes observed GFP+ cell bodies surrounded by PV+ varicosities. I: Parvalbumin staining of the same region shown in C–E. J: Merged images of GFP and parvalbumin immunostaining. Scale bars = 20 μm in A (applies to B,C); 50 μm in D; 30 μm in J (applies to E–G,I; 15 μm in H).

DISCUSSION

Although the avian and mammalian forebrains differ at the level of gross morphology, several lines of evidence suggest that the basic cell types, and perhaps circuitry, are conserved between birds and mammals. Our results suggest that postnatal neurogenesis in the songbird shares some important similarities to embryonic neurogenesis in birds and mammals. Based on the expression of the transcription factors TBR1, DLX, NKX2.1, and ISL-1/2, it appears that the same pattern of gene expression present in the lateral ventricle of embryonic mice and chicks (Puelles et al., 2000; Stenman et al., 2003) persists in the brains of juvenile zebra finches. Moreover, we have demonstrated that in juvenile zebra finches these regions of the lateral ventricle produce similar neuronal subtypes to those generated from homologous regions of the embryonic mouse (Marin and Rubenstein, 2003; Xu et al., 2004; Butt et al., 2005). We observed the addition of at least four different classes of new neurons to the song system of the juvenile zebra finch: 1) HVC to RA projection cells, 2) spiny, PV−, GABA+ neurons in HVC, 3) aspiny PV+, GABA+ neurons in HVC, and 4) medium spiny neurons in Area X, two of which, medium spiny neurons and PV+ inhibitory interneurons, have clear homologs in the mammalian forebrain.

Identity of cells targeted by oncoretroviral vectors

Oncoretroviral vectors are capable of infecting mitotically active cells, therefore it is somewhat surprising that we did not observe any GFP+ radial glia in the injection site, since these cells are know to be actively dividing stem cells that give rise to new neurons in the vertebrate forebrain (Alvarez-Buylla et al., 1990b; Noctor et al., 2001). Moreover, we did not observe any GFP+ cells remaining in the VZ after long (35 days) survival times. These obser-

vations suggest that we are not infecting the true stem cells that reside in the VZ, and instead are infecting either a progenitor that gives rise to migrating neuroblasts or the neuroblasts themselves during mitosis. Similar observations have been made following oncoretroviral injections into the subventricular zone of newborn mice, where the oncoretrovirus appears to infect newborn cells that migrate to the olfactory bulb, but not the stem cells within the walls of the lateral ventricle (Luskin, 1993).

Origin of HVC_{RA} projection neurons

Previous studies using a combination of retrograde tracing from RA and ^3H thymidine labeling identified the majority of HVC neurons born after hatching as HVC_{RA} neurons (Nordeen and Nordeen, 1988; Alvarez-Buylla et al., 1988a, 1990a). Our results confirm the addition of HVC_{RA} neurons into the juvenile finch brain and identify the VZ above HVC as their site of origin, as suggested by Goldman and Nottebohm (1983). Our data suggest that the VZ above HVC is the only region of the VZ that generates HVC_{RA} neurons during vocal learning. However, this region of the V2 may also produce other types of neurons exclusively for HVC, as there were, after all injections; GFP+ cells in the nearby nidopallium.

Since the juvenile zebra finch VZ above HVC appears to generate HVC_{RA} projection neurons, but not neurons that project to Area X or interneurons, it should be possible to specifically target this cell type by infection of the precursor cells with an oncoretroviral vector. In this study we introduced GFP into a subset of HVC_{RA} neurons. However, oncoretroviral vectors can be engineered to carry an expression cassette containing any gene of interest. Genes of interest can also be introduced into fully mature HVC_{RA} neurons by direct infection of HVC with lentiviral-based vectors (B.B.S., unpubl. obs.), a class of vectors that can infect both postmitotic cells as well as cells that are actively proliferating (Naldini et al., 1996). However, this method would also target other neuronal cell types in HVC, such as interneurons and HVC to Area X projection cell, as well as nonneuronal cell types, such as astrocytes.

Origin of HVC GABAergic interneurons

Our results also identify the site of interneuron origin for HVC. Following oncoretroviral injections into the ventral VZ we observed at least two classes of GABAergic interneurons in HVC. These cells may migrate to their destination in the song circuit by tangential migration, a form of migration independent of radial glia used by interneuron precursors in the mammalian forebrain (Anderson et al., 1997).

Of the two classes of new HVC interneurons we observed, the addition of PV+ aspiny cells is particularly interesting. These cells resemble the fast-spiking PV+ basket cells of the mammalian cortex and hippocampus in terms of morphology, electrophysiology, immunohistochemistry, and developmental origin. In mammals, fast-spiking basket cells are thought to contribute to precise spike timing (Pouille and Scanziani, 2001). PV+ aspiny cells in HVC have been shown to mediate fast feedforward inhibition onto projection neurons and interneurons (Mooney and Prather, 2005). The firing patterns of interneurons and projection neurons of the song system during song-related activity have submillisecond temporal precision (Yu and Margoliash, 1996; Chi and Margoliash, 2001; Hahnloser et al., 2002), and perhaps PV+ aspiny cells in HVC contribute to the precision of this timing. PV+ basket cells have also been implicated in the control of the critical period of ocular dominance plasticity in the mammalian visual cortex (Hensch, 2005). It would be of considerable interest if the addition of PV+ interneurons into the juvenile brain had a similar role in the sensitive period for vocal learning.

It is more difficult to speculate on the function of the spiny, PV−, GABAergic interneurons in HVC because their electrophysiology has not been characterized.

Nature and role of the new Area X neurons

Postnatal new neuron addition occurs in songbirds at its highest rate in Area X and the surrounding striatum (Alvarez-Buylla et al., 1994). We were able to identify these new cells as medium spiny neurons (MSNs), the principal neurons of the vertebrate striatum. This result is somewhat surprising. While the circuitry and cell type composition of the basal ganglia appears conserved between mammals and birds (Doupe et al., 2005), MSNs were only recently identified in avian striatum (Farries and Perkel, 2000). MSNs are a major component of the mammalian basal ganglia and have attracted a great deal of interest because these cells are preferentially lost in Huntington's disease (Mitchell et al., 1999).

The addition of MSNs may be related to vocal learning. Area X is the input structure to the anterior forebrain pathway (AFP), a neural pathway essential for song learning, but not for the production of learned song (Bottjer et al., 1984). MSNs are thought to be the primary input cells in Area X, and therefore the AFP, receiving direct synaptic input from both HVC and LMAN (Farries et al., 2005). The AFP has been hypothesized to control the variability of the juvenile song and may provide a means for songbirds to explore a range of vocalizations (Kao et al., 2005; Olveczky et al., 2005); however, the precise function of Area X in song learning has been difficult to determine. One intriguing hypothesis is that Area X may be involved in the acquisition of the tutor's song (Ding and Perkel, 2004; Singh et al., 2005). Perhaps new medium spiny neurons are involved in the formation of new auditory memories that are used to shape the output of the AFP during singing (Solis and Doupe, 2000).

Comparative neuroanatomy based on cell type

Historically, comparative vertebrate neuroanatomy has focused on the homologies between similar brain regions found in different vertebrate species (Nieuwenhuys et al., 1998). However, evidence from fate mapping experiments and mouse mutants has shown that a single forebrain region is composed of a variety of cells types, each derived from a distinct lineage (Marin and Rubenstein, 2003). Moreover, it has been observed that anatomically distinct brain regions, such as the striatum, neocortex, amygdala, and hippocampus, contain neurons, particularly interneurons, that share the same developmental origin (Marin et al., 2000; Reid and Walsh, 2002; Nery et al., 2002; Xu et al., 2004) and have very similar physiological properties. Since cell types appear to be shared across anatomically distinct brain areas within a species and across similar brain areas in different vertebrate species, it seems important to consider the cell type as a conserved unit that may have similar functions in different neural circuits.

Our experiments provide evidence that cells in the vocal learning circuit of the avian forebrain share a strong homology to cell types found in the mammalian cortex and basal ganglia. Previous studies have suggested the existence of similar cell types in the avian and mammalian forebrain based on morphological, electrophysiological, and immunohistochemical evidence (Wild et al., 1993; Farries and Perkel, 2000; Mooney and Prather, 2005). Based on similarities of cell connectivity, it has been hypothesized that although the avian and mammalian forebrains differ at the level of gross anatomy, they share equivalent circuits (Karten, 1997; Jarvis et al., 2005). We propose that different cell types in the vertebrate brain may have evolved to perform certain computations in a neural circuit, and that a particular cell type can be used in different brain regions where its specialized function is needed. Taking a comparative approach across different taxa may help to identify the function of specific cell types of the forebrain. The existence of specialized brain circuits for learning a robust quantifiable behavior makes the nervous system of songbirds a particularly attractive system for exploring the functional contribution of different neuronal types.

LITERATURE CITED

Alvarez-Buylla A, Nottebohm F. 1988. Migration of young neurons in adult avian brain. Nature 335:353–354.

Alvarez-Buylla A, Theelen M, Nottebohm F. 1988a. Birth of projection neurons in the higher vocal center of the canary forebrain before, during, and after song learning. Proc Natl Acad Sci U S A 85:8722–8726.

Alvarez-Buylla A, Theelen M, Nottebohm F. 1988b. Mapping of radial glia and of a new cell type in adult canary brain. J Neurosci 8:2707–2712.

Alvarez-Buylla A, Kirn JR, Nottebohm F. 1990a. Birth of projection neurons in adult avian brain may be related to perceptual or motor learning. Science 249:1444–1446.

Alvarez-Buylla A, Theelen M, Nottebohm F. 1990b. Proliferation "hot spots" in adult avian ventricular zone reveal radial cell division. Neuron 5:101–109.

Alvarez-Buylla A, Ling CY, Yu WS. 1994. Contribution of neurons born during embryonic, juvenile, and adult life to the brain of adult canaries: regional specificity and delayed birth of neurons in the song-control nuclei. J Comp Neurol 347:233–248.

Alvarez-Buylla A, Garcia-Verdugo JM, Mateo AS, Merchant-Larios H. 1998. Primary neural precursors and intermitotic nuclear migration in the ventricular zone of adult canaries. J Neurosci 18:1020–1037.

Anderson KD, Reiner A. 1991. Immunohistochemical localization of DARPP-32 in striatal projection neurons and striatal interneurons: implications for the localization of D1-like dopamine receptors on different types of striatal neurons. Brain Res 568:235–243.

Anderson SA, Eisenstat DD, Shi L, Rubenstein JL. 1997. Interneuron migration from basal forebrain to neocortex: dependence on Dlx genes. Science 278:474–476.

Bottjer SW, Miesner EA, Arnold AP. 1984. Forebrain lesions disrupt development but not maintenance of song in passerine birds. Science 224:901–903.

Brown ST, Wang J, Groves AK. 2005. Dlx gene expression during chick inner ear development. J Comp Neurol 483:48–65.

Butt SJ, Fuccillo M, Nery S, Noctor S, Kriegstein A, Corbin JG, Fishell G. 2005. The temporal and spatial origins of cortical interneurons predict their physiological subtype. Neuron 48:591–604.

Chi Z, Margoliash D. 2001. Temporal precision and temporal drift in brain and behavior of zebra finch song. Neuron 32:899–910.

Cobos I, Puelles L, Martinez S. 2001. The avian telencephalic subpallium originates inhibitory neurons that invade tangentially the pallium (dorsal ventricular ridge and cortical areas). Dev Biol 239:30–45.

Deacon TW, Pakzaban P, Isacson O. 1994. The lateral ganglionic eminence is the origin of cells committed to striatal phenotypes: neural transplantation and developmental evidence. Brain Res 668:211–219.

Dewulf V, Bottjer SW. 2005. Neurogenesis within the juvenile zebra finch telencephalic ventricular zone: a map of proliferative activity. J Comp Neurol 481:70–83.

Ding L, Perkel DJ. 2004. Long-term potentiation in an avian basal ganglia nucleus essential for vocal learning. J Neurosci 24:488–494.

Doupe AJ, Perkel DJ, Reiner A, Stern EA. 2005. Birdbrains could teach basal ganglia research a new song. Trends Neurosci 28:353–363.

Farries MA, Perkel DJ. 2000. Electrophysiological properties of avian basal ganglia neurons recorded in vitro. J Neurophysiol 84:2502–2513.

Farries MA, Perkel DJ. 2002. A telencephalic nucleus essential for song learning contains neurons with physiological characteristics of both striatum and globus pallidus. J Neurosci 22:3776–3787.

Farries MA, Ding L, Perkel DJ. 2005. Evidence for "direct" and "indirect" pathways through the song system basal ganglia. J Comp Neurol 484:93–104.

Goldman SA, Nottebohm F. 1983. Neuronal production, migration, and differentiation in a vocal control nucleus of the adult female canary brain. Proc Natl Acad Sci U S A 80:2390–2394.

Hahnloser RH, Kozhevnikov AA, Fee MS. 2002. An ultra-sparse code underlies the generation of neural sequences in a songbird. Nature 419:65–70.

Hemmings HC Jr, Greengard P. 1986. DARPP-32, a dopamine- and adenosine 3′:5′-monophosphate-regulated phosphoprotein: regional, tissue, and phylogenetic distribution. J Neurosci 6:1469–1481.

Hensch TK. 2005. Critical period plasticity in local cortical circuits. Nat Rev Neurosci 6:877–888.

Hevner RF, Hodge RD, Daza RA, Englund C. 2006. Transcription factors in glutamatergic neurogenesis: conserved programs in neocortex, cerebellum, and adult hippocampus. Neurosci Res 55:223–233.

Hsueh YP, Wang TF, Yang FC, Sheng M. 2000. Nuclear translocation and transcription regulation by the membrane-associated guanylate kinase CASK/LIN-2. Nature 404:298–302.

Jarvis ED, Gunturkun O, Bruce L, Csillag A, Karten H, Kuenzel W, Medina L, Paxinos G, Perkel DJ, Shimizu T, Striedter G, Wild JM, Ball GF, Dugas-Ford J, Durand SE, Hough GE, Husband S, Kubikova L, Lee DW, Mello CV, Powers A, Siang C, Smulders TV, Wada K, White SA, Yamamoto K, Yu J, Reiner A, Butler AB. 2005. Avian brains and a new understanding of vertebrate brain evolution. Nat Rev Neurosci 6:151–159.

Kao MH, Doupe AJ, Brainard MS. 2005. Contributions of an avian basal ganglia-forebrain circuit to real-time modulation of song. Nature 433:638–643.

Karten HJ. 1997. Evolutionary developmental biology meets the brain: the origins of mammalian cortex. Proc Natl Acad Sci U S A 94:2800–2804.

Kawaguchi Y, Kubota Y. 1996. Physiological and morphological identification of somatostatin- or vasoactive intestinal polypeptide-containing cells among GABAergic cell subtypes in rat frontal cortex. J Neurosci 16:2701–2715.

Kirn JR, Alvarez-Buylla A, Nottebohm F. 1991. Production and survival of projection neurons in a forebrain vocal center of adult male canaries. J Neurosci 11:1756–1762.

Kirn JR, Fishman Y, Sasportas K, Alvarez-Buylla A, Nottebohm F. 1999. Fate of new neurons in adult canary high vocal center during the first 30 days after their formation. J Comp Neurol 411:487–494.

Lois C, Hong EJ, Pease S, Brown EJ, Baltimore D. 2002. Germline transmission and tissue-specific expression of transgenes delivered by lentiviral vectors. Science 295:868–872.

Luskin MB. 1993. Restricted proliferation and migration of postnatally generated neurons derived from the forebrain subventricular zone. Neuron 11:173–189.

Marin O, Rubenstein JL. 2003. Cell migration in the forebrain. Annu Rev Neurosci 26:441–483.

Marin O, Anderson SA, Rubenstein JL. 2000. Origin and molecular specification of striatal interneurons. J Neurosci 20:6063–6076.

Markram H, Toledo-Rodriguez M, Wang Y, Gupta A, Silberberg G, Wu C. 2004. Interneurons of the neocortical inhibitory system. Nat Rev Neurosci 5:793–807.

Mitchell IJ, Cooper AJ, Griffiths MR. 1999. The selective vulnerability of striatopallidal neurons. Prog Neurobiol 59:691–719.

Mooney R, Prather JF. 2005. The HVC microcircuit: the synaptic basis for interactions between song motor and vocal plasticity pathways. J Neurosci 25:1952–1964.

Naldini L, Blomer U, Gallay P, Ory D, Mulligan R, Gage FH, Verma IM, Trono D. 1996. In vivo gene delivery and stable transduction of nondividing cells by a lentiviral vector. Science 272:263–267.

Nery S, Fishell G, Corbin JG. 2002. The caudal ganglionic eminence is a source of distinct cortical and subcortical cell populations. Nat Neurosci 5:1279–1287.

Nieuwenhuys R, Donkelaar HJt, Nicholson C. 1998. The central nervous system of vertebrates. Berlin: Springer.

Nixdorf BE, Davis SS, DeVoogd TJ. 1989. Morphology of Golgi-impregnated neurons in hyperstriatum ventralis, pars caudalis in adult male and female canaries. J Comp Neurol 284:337–349.

Noctor SC, Flint AC, Weissman TA, Dammerman RS, Kriegstein AR. 2001. Neurons derived from radial glial cells establish radial units in neocortex. Nature 409:714–720.

Nordeen KW, Nordeen EJ. 1988. Projection neurons within a vocal motor pathway are born during song learning in zebra finches. Nature 334: 149–151.

Nordeen EJ, Nordeen KW. 1990. Neurogenesis and sensitive periods in avian song learning. Trends Neurosci 13:31–36.

Nottebohm F. 1999. The anatomy and timing of vocal learning in birds. In: Hauser MD, Konishi M, editors. The design of animal communication. Cambridge, MA: MIT Press. p 63–110.

Nottebohm F. 2002. Why are some neurons replaced in adult brain? J Neurosci 22:624–628.

Nottebohm F. 2004. The road we travelled: discovery, choreography, and significance of brain replaceable neurons. Ann N Y Acad Sci 1016:628–658.

Olveczky BP, Andalman AS, Fee MS. 2005. Vocal experimentation in the juvenile songbird requires a basal ganglia circuit. PLoS Biol 3:e153.

Panganiban G, Sebring A, Nagy L, Carroll S. 1995. The development of crustacean limbs and the evolution of arthropods. Science 270:1363–1366.

Parra P, Gulyas AI, Miles R. 1998. How many subtypes of inhibitory cells in the hippocampus? Neuron 20:983–993.

Paton JA, Nottebohm FN. 1984. Neurons generated in the adult brain are recruited into functional circuits. Science 225:1046–1048.

Pouille F, Scanziani M. 2001. Enforcement of temporal fidelity in pyramidal cells by somatic feed-forward inhibition. Science 293:1159–1163.

Puelles L, Kuwana E, Puelles E, Bulfone A, Shimamura K, Keleher J, Smiga S, Rubenstein JL. 2000. Pallial and subpallial derivatives in the embryonic chick and mouse telencephalon, traced by the expression of the genes Dlx-2, Emx-1, Nkx-2.1, Pax-6, and Tbr-1. J Comp Neurol 424:409–438.

Reid CB, Walsh CA. 2002. Evidence of common progenitors and patterns of dispersion in rat striatum and cerebral cortex. J Neurosci 22:4002–4014.

Reiner A, Perera M, Paullus R, Medina L. 1998. Immunohistochemical localization of DARPP32 in striatal projection neurons and striatal interneurons in pigeons. J Chem Neuroanat 16:17–33.

Roe T, Reynolds TC, Yu G, Brown PO. 1993. Integration of murine leukemia virus DNA depends on mitosis. EMBO J 12:2099–2108.

Singh TD, Nordeen EJ, Nordeen KW. 2005. Song tutoring triggers CaMKII phosphorylation within a specialized portion of the avian basal ganglia. J Neurobiol 65:179–191.

Sohrabji F, Nordeen EJ, Nordeen KW. 1993. Characterization of neurons born and incorporated into a vocal control nucleus during avian song learning. Brain Res 620:335–338.

Solis MM, Doupe AJ. 2000. Compromised neural selectivity for song in birds with impaired sensorimotor learning. Neuron 25:109–121.

Somogyi P, Klausberger T. 2005. Defined types of cortical interneurone structure space and spike timing in the hippocampus. J Physiol 562: 9–26.

Stenman J, Toresson H, Campbell K. 2003. Identification of two distinct progenitor populations in the lateral ganglionic eminence: implications for striatal and olfactory bulb neurogenesis. J Neurosci 23:167–174.

Stokes TM, Leonard CM, Nottebohm F. 1974. The telencephalon, diencephalon, and mesencephalon of the canary, *Serinus canaria*, in stereotaxic coordinates. J Comp Neurol 156:337–374.

Tsuchida T, Ensini M, Morton SB, Baldassare M, Edlund T, Jessell TM, Pfaff SL. 1994. Topographic organization of embryonic motor neurons defined by expression of LIM homeobox genes. Cell 79:957–970.

Wang TF, Ding CN, Wang GS, Luo SC, Lin YL, Ruan Y, Hevner R, Rubenstein JL, Hsueh YP. 2004. Identification of Tbr-1/CASK complex target genes in neurons. J Neurochem 91:1483–1492.

Wichterle H, Turnbull DH, Nery S, Fishell G, Alvarez-Buylla A. 2001. In utero fate mapping reveals distinct migratory pathways and fates of neurons born in the mammalian basal forebrain. Development 128: 3759–3771.

Wilbrecht L, Williams H, Gangadhar N, Nottebohm F. 2006. High levels of new neuron addition persist when the sensitive period for song learning is experimentally prolonged. J Neurosci 26:9135–9141.

Wild JM, Karten HJ, Frost BJ. 1993. Connections of the auditory forebrain in the pigeon (*Columba livia*). J Comp Neurol 337:32–62.

Wild JM, Williams MN, Howie GJ, Mooney R. 2005. Calcium-binding proteins define interneurons in HVC of the zebra finch (*Taeniopygia guttata*). J Comp Neurol 483:76–90.

Wilson CJ. 2004. Basal ganglia. In: Shepherd GM, editor. The synaptic organization of the brain, 5th ed. Oxford: Oxford University Press. p 361–413.

Xu Q, Cobos I, De La Cruz E, Rubenstein JL, Anderson SA. 2004. Origins of cortical interneuron subtypes. J Neurosci 24:2612–2622.

Yamamoto T, de Crombrugghe B, Pastan I. 1980. Identification of a functional promoter in the long terminal repeat of Rous sarcoma virus. Cell 22:787–797.

Yu AC, Margoliash D. 1996. Temporal hierarchical control of singing in birds. Science 273:1871–1875.

Chapter 3

Search-like Neuronal Migration in the Postnatal Vertebrate Forebrain

Most vertebrate species add new neurons to brain circuits throughout life, a process thought to be essential for tissue maintenance, repair and learning. How new neurons migrate through the mature brain, differentiate into neurons and establish synaptic connections within a functioning circuit is not know. We used two-photon microscopy to image the addition of genetically labeled newly generated neurons into the brain of juvenile zebra finches. Time-lapse *in vivo* imaging revealed that the majority of new neurons were morphologically complex, extending several motile processes in different directions, and migrated hundreds of microns over multiple days. These cells lacked obvious polarity and switched direction frequently by nuclear invasion of a new process. Migration frequently ended only after new cells made direct soma-soma contact with mature neurons. These results provide direct, *in vivo* evidence for a search-like form of neuronal migration involved in the addition of new neurons into the postnatal brain.

The migration and integration of new neurons into brain circuits is an essential process in vertebrate development. In humans and other mammals, this process is mostly complete before or soon after birth, except in two brain regions, the hippocampus[1,2] and olfactory bulb[3,4], where new neurons continue to be added throughout life. In contrast, widespread postnatal neurogenesis is found in most other vertebrate species, including fish, amphibians, reptiles and birds[5]. Since its discovery, postnatal neurogenesis has stimulated interest as a potential therapeutic treatment for brain disorders caused by neuronal loss[6]. The successful implementation of this strategy will require understanding how new neurons migrate through the mature brain and integrate into existing circuits without disrupting behavior.

Songbirds are a leading model system for the study of postnatal neurogenesis because they add new neurons into the song system, a specialized forebrain circuit that controls the production of the song[7]. One nucleus in the song system, the High Vocal Center (HVC), receives new excitatory neurons that project to downstream motor nuclei and form a pathway that is essential for normal singing[8]. Interestingly, in two songbird species, zebra finches and canaries, the highest rate of neurogenesis in HVC occurs during the critical period for song learning[9,10], suggesting that the addition of new

neurons is essential for memory formation. However, the mechanisms by which new cells reach HVC, differentiate into neurons and form synaptic connections in HVC during song learning are unknown.

Multiple forms of neuron migration have been described in the vertebrate brain[11-12]. For instance, in the embryonic mammalian cortex, projection neurons use the fibers of radial glia as a scaffold for their migration[13] whereas interneurons are closely associated with corticofugal axons[14]. In birds, radial fibers persist into adulthood, suggesting that these may guide postnatal neuron migration as well[15]. However, radial fibers are sparse or absent in HVC, suggesting that other mechanisms of neuron migration may exist[16]. To address these questions we used real time, *in vivo* imaging to directly observed the migration and integration of new neurons into the HVC of juvenile zebra finches.

Results

Multiple migratory neuronal types in the postnatal brain

To selectively image newly born neurons in HVC, we labeled the progenitor cells for HVC neurons in 40-60 day old zebra finch males with a GFP encoding oncoretroviral vector, which only infects mitotically active cells[17]. At 8 days post infection (dpi), soon after new neurons begin to enter HVC[18,19], we observed two main GFP+ cell types in tissue sections from HVC. Thirty percent (14/52) of the GFP labeled cells had a morphology that corresponded to the classically described bipolar migratory neurons[20], and were frequently (10/14) associated with radial glia (Fig. 1a). In contrast, the majority of GFP+ cells within HVC (38/52) had a complex morphology with three to eight (mean=4.0) processes extending in multiple directions from the cell body (Fig. 1b), and were infrequently (3/38) associated with radial glia. Most complex cells within HVC expressed Hu (70/75) (a marker for neurons at all developmental stages)[19] and Dcx (50/75) (a marker for migratory and immature, post-migratory neurons)[21,22], but few expressed NeuN (1/75) (a marker for mature neurons)[23] (suppl figs. a-c) suggesting that complex cells, while committed to a neuronal fate, may not have completed their migration.

Migratory behavior of new neurons *in vivo*

To examine the behavior of complex cells *in vivo*, we performed two-photon time-lapse imaging on GFP+ cells in HVC beginning at 7 dpi. Since HVC is a superficial brain structure extending from 100μm to 700μm below the pial surface, it was possible to image the complete migratory trajectories of newly generated cells *in vivo* for up to three weeks. GFP+ cells were initially tracked at 12-hour intervals until they stopped moving or left the field of view (700 μm x 1000 μm x 200 μm depth). To accurately identify the positions of GFP+ cells across successive imaging sessions we retrogradely labeled HVC_x cells, a neuronal population in HVC projecting to Area X of the avian striatum that is generated exclusively during the embryonic period, using the fluorescent marker DiI (Fig. 1d). The position of the DiI labeled HVC_x neurons relative to each other did not change over time and could be used to register imaging fields across successive imaging sessions (see methods).

In vivo the majority of GFP+ HVC cells (19/21) lacked obvious polarity, and had multiple processes extending in different directions, closely resembling the complex GFP+ cells observed in histologically processed tissue sections (Fig. 1c). Time-lapse imaging revealed that these cells were migratory neurons, moving their somata up to 126 μm in a 12-hour period (mean +/- s.d. = 42.6 +/- 27.1μm). Two features of the migratory behavior of these cells were surprising and deviated from previously described forms of migration. First, complex cells did not migrate along straight paths; instead they frequently changed directions (Fig. 1e). As a result, the tortuosity (τ) of their trajectories, defined as the ratio between path length and the distance between the path's start and end points, was high (τ=1.69 +/-0.81). Second, cells changed morphology significantly between imaging sessions, adding and removing most of their processes (Fig. 1f). In contrast to the behavior of complex cells, time-lapse imaging revealed that bipolar cells in HVC (n=2) had migratory routes of low tortuosity (τ =1.06 and 1.13), consistent with their presumed association with the radial glia scaffold. We also compared the migration paths of 11 complex GFP+ cells with the pattern of blood vessels, another scaffold for migrating neurons[24]. None (0/11) of the complex cells followed the pattern of blood vessels (suppl fig. d) suggesting that these newly generated cells did not use blood vessels as scaffold for their migration.

Mechanisms of complex cell migration

To investigate migratory mechanisms at a finer timescale we acquired time-lapse images of HVC every 6 minutes for up to 6 hours. Analysis of soma movements revealed that complex cells (n=7) moved up to 0.6 μm per minute (mean= 0.14 +/- 0.12 μm/min) and changed directions every 152 minutes on average (+/-54 min) (mean turn angle= 68°, +/-36°, see methods). Movement of the cell body always (12/12 movements, 7 cells) occurred by translocation of the nucleus along one of the processes emanating from the cell body (Fig. 2a). Direction change was accomplished by the cell nucleus invading a process whose heading differed from the previous trajectory (Fig. 2b). Before the invasion of a new process the movement of the cell body would cease, resulting in alternating periods of movement and rest during the course of migration (Fig. 2c-e). The movements of all GFP+ cells were biased away from the lateral ventricle (mean elevation = -11.57°, $P<0.001$ Rayleigh test, see methods) (Suppl Fig. f), but exhibited no other directional preference. Their trajectories were uniformly distributed in the horizontal plane ($P=0.066$, Rayleigh test) (suppl Fig. g). If migrating cells in HVC were following a chemoattractant gradient one would expect cell headings to be biased towards the source of the gradient. The multiple migratory directions of GFP+ cells within HVC suggests that new neurons are not guided by a single point source of chemoattractant. Instead the data are consistent with the existence of a chemorepellent, present in the VZ, which drives cells away from lateral ventricle and into the brain parenchyma.

To assess the effects of anesthesia on the migratory behavior of immature neurons we measured the displacement rates of cells imaged in animals continually anesthetized for 6 hours, and compared them with those of cells in animals returned to their cages between imaging sessions. We used displacement rate, defined as the direct distance between a cell's start and end position over a defined time interval, because the instantaneous velocities and turn frequencies could not be calculated for cells imaged at 3 and 12-hour intervals. We observed no significant difference in displacement rates over a 3-hour interval between cells imaged in anesthetized animals (n=7 cells) and cells from animals returned to their cages between imaging sessions (n= 11 cells) (2-sided t-test, $p=0.8238$).

The processes of complex cells were dynamic (Fig. 3a, 3b) and appeared to sample the cell's immediate environment. The process tips grew and retracted at equal speed (0.67 +/- 0.64 μm/min). On average, processes oriented in the direction of movement (see methods) experienced significantly more growth than process oriented in other directions (two-tailed, two-sample t-test $p<0.001$) (Fig. 3c). Processes undergoing growth had a swelling at their distal tip that was absent from retracting processes (Fig. 3a). These swellings resembled axonal growth cones and were frequently observed making contact with the somata of mature neurons (Fig. 3d), perhaps reflecting a sensory role for process tips.

To determine the eventual developmental fate of these complex migratory cells, we imaged GFP+ cells (n=66) at 48-hour intervals. Once cells had ceased migrating (n=16/66) we were able to monitor their differentiation into mature neurons up to 30 dpi. Based on morphological evidence, including the presence of dendrites, dendritic spines and an axon, all 16 GFP+ cells that stopped migrating in HVC appeared to differentiate into neurons. Of these cells, 75% (12/16) made soma-soma contact with HVC_X neurons. In contrast, only 24% (12/50) of the GFP+ cells that subsequently continued migrating over the next imaging session made soma-soma contact with HVC_X cells. These observations suggest that mature HVC neurons may provide cues for the termination of neuronal migration.

Discussion

Using *in vivo* two-photon imaging, we have observed a previously undescribed search-like form of migration involved in the construction of a neural circuit in the postnatal brain during learning. The behavior and morphology of these migratory cells suggests that they do not follow a predetermined route or scaffold. Complex cells in HVC extend multiple processes in different directions and then select one of these processes to transiently determine their heading. In other brain regions new neurons that migrate along a scaffold have a simple, polar morphology that reflects the commitment of those cells to a particular route[25]. The existence of multiple, exploratory processes emanating from the somata of migratory neuroblasts within HVC suggests a flexibility of

direction that is not consistent with a cell's heading being predetermined by a fixed scaffold guiding its migration.

Migrating neuron reminiscent of complex cells in HVC have been described in tissue slices from the embryonic cortex *in vitro*[26,27,28,29]. In these reports newborn neurons with multiple processes were reported to move in an undirected, random walk or "wandering" pattern. However it is unclear if this wandering form of migration plays a role in brain development, or whether it may be an artifact of the *in vitro* slice preparation used[29]. Our results confirm the existence of a search-like form of migration in the intact postnatal brain. This observation supports the hypothesis that wandering migration plays a general role in the assembly of neuronal circuits, including the mammalian neocortex.

The behavior of migratory cells in HVC indicates the existence of a cellular mechanism that allows new neurons to navigate through the mature brain. One of the bottlenecks for successful neuron replacement strategies for the treatment of neurological disease is the inefficient migration observed when cells are grafted into the mature mammalian brain. This limitation appears to be due not to the lack of permissivity of the adult parenchyma, but by the intrinsic inability of most grafted cells to migrate[30] in the absence of specific scaffolds. The activation of the cellular program responsible for the search-like migration we have observed may allow grafted cells to integrate into the mature human brain to replace cells lost to injury or disease.

Methods

Virus Production

Membrane-targeted GFP, a fusion of GFP with the palmitolation sequence from the N terminus of Gap-43[31], was cloned into an oncoretroviral vector, based on the Moloney Murine Leukemia virus. GFP expression was driven by the internal promoter of the Rous Sarcoma Virus, which we had previously shown to be a strong promoter in migrating neurons in the Zebra Finch[32]. Viral particles were produced as described[33], and concentrated to 0.5-1.5 X 10^6 infectious units per microliter. Aliquots of viral vector were stored at -80°C until use.

Subjects

All experiments were carried out in accordance with protocols approved by the Committee on Animal Care at the Massachusetts Institute of Technology. Data were Twenty-five Juvenile zebra finch males (44-72 days old) from our breeding colony at MIT were used for this study.

Surgical Procedure and Animal Care

At age 38-45 days, birds were removed from the breeding colony and underwent stereotaxic surgery. Anesthesia was maintained with 1-2% isoflurane in air. Birds for immuno-histochemical analysis received 2mm diameter craniotomies dorsal to HVC on the right hemisphere. Injections of GFP-carrying viral vector (600-900nl total volume) were targeted to the ventricular zone dorsal to HVC, which lies 0.0mm anterior, 2.1mm lateral of the bifurcation of the sagital sinus and 0.1-0.2mm bellow the dura. Following recovery, finches were housed with other males in our aviary.

Surgery to prepare animals for *in vivo* imaging was the same as above except for the following modifications: 1M mannitol (20μl/g) was administered to decrease intracranial pressure and reduce bleeding during surgery. Larger craniotomies, 3-4mm in diameter, were made above HVC to accommodate the chronic implant. Care was taken to minimize bleeding of the dura surface. Following skull removal and viral injections, a thin layer of transparent biocompatible silicone (Kwik-Sil, WPI) was applied to the dura and a cover glass was placed on top. We began experiments with 5mm diameter cover glass (1943-00005, Bellco Glass) and switched to 3mm diameter cover glass (3mm circular, #0, Corning 0211 borosilicate glass, Thermo-Fisher Scientific). We noticed no difference in the clarity of the optical implant or health of the animal between glass types, but found surgery more successful with smaller craniotomies. Optical-curing dental cement (Pentron Clinical Technologies) was used to affix the cover glass to the skull. A small steel plate (4.75 x 2.25 x 1.00 mm) with threaded screw holes was imbedded in the dental cement, allowing the head to be temporarily mounted onto the microscope stage to maintain head placement during imaging. Birds also received 50nl injections of DiI (Molecular Probes), 5mg/ml in Dimethylformamide (Sigma), into area X. Following

surgery, and between imaging sessions a small amount of opaque biocompatible silicone (Kwik-Cast, WPI) was applied to the cover glass to protect the glass from debris and the brain from light. Birds were housed individually in acoustically-isolated chambers. Songs were recorded in some birds to verify that the optical window, surgery and repeated anesthesia did not disrupt normal development. Birds were kept on 12h:12h or 16h:8h light:dark schedules.

Histology and Immunocytochemistry

Histological procedures are similar to those described previously[32]. Eight days after injection with retroviral vectors, animals were deeply anesthetized and perfused with 3% paraformaldehyde (Sigma). After removal from the skull, brains were post-fixed in 3% paraformaldehyde overnight at 4C. Tissue sections were cut with a vibrating microtome (Leica) 40μm thick. Sections containing HVC were incubated in blocking solution, 2% milk, 0.25% triton in PBS, for 20 minutes at room temperature and then transferred to primary antibody solution which included rabbit anti-GFP (AB3080, Chemicon) diluted 1:400 in blocking solution and a second primary (see bellow for list of antibodies and dilutions) in blocking solution and incubated incubated overnight at 4C. Sections were washed 3 times in PBS for 45 min total, then transferred to secondary antibody solution, Alexa Fluor 488 goat anti-rabbit IgG (A11008, Molecular Probes) and Alexa Fluor 555 donkey anti-goat IgG (A21432, Molecular Probes) and Alexa Fluor 647 goat anti-mouse IgM (A21238, Molecular Probes) both diluted 1:750 in blocking solution, incubated 2 hours at room temperature, washed as before and mounted. Imaging was performed with an Olympus Fluoview confocal microscope and analyzed with ImageJ.

To examine the relationship between neuroblasts and radial glia, sections were stained for vimentin using 40E-C supernatant (Developmental Studies Hybridoma Bank, University of Iowa) diluted 1:10. Dcx was detected using a goat polyclonal antibody (diluted in blocking solution 1:500) (sc8066, Santa Cruz Biotechnology). Hu was detected using a mouse monoclonal antibody (diluted in blocking solution 1:25) (A21271, lot 71C1-1, Molecular Probes). NeuN was detected using a mouse monoclonal antibody (diluted in blocking solution 1:500) (Chemicon, Temecula, CA; MAB377, lot 19060600)

Two-photon Microscope

Imaging was performed on a custom-built two-photon laser-scanning microscope. GFP and DiI positive cells were excited by near infrared light (960nm) produced by a Ti:sapphire laser (Tsunami, Spectra Physics) pumped by a 10-W solid-state laser. Images were acquired using a 20x 0.95 NA water immersion objective lens (Olympus) and photomultiplier tubes (H7422, Hamamatsu).

Time-lapse imaging

Beginning six to eight days after surgery animals were anesthetized with 0.8-1.2% isoflurane in oxygen, and head fixed under the two-photon microscope objective. The birds rested on a pad heated to 42°C, the microscope objective and head-post were also heated to 42°C. To produce movies of migration (n= 2 birds) images were acquired every 6 minutes for up to 6 hours. Imaging was performed during night hours, which allowed us to use lower concentrations of isoflurane (~0.8%) to maintain anesthesia. The immersion fluid above the objective was heated to 34-36°C. Other birds were imaged every 48 hours (12 birds), 12 hours (2 birds), and 3 hours (2 birds). The duration of imaging sessions ranged from 30-45 minutes. Between imaging sessions animals were housed singly or in pairs.

Labeling Blood vessels

To test whether blood vessels formed a scaffold for migration in HVC we recorded the positions of GFP+ cells every 3 hours for 15-18 hours. To label blood vessels we injected 50ul of 20mM Sulforhodamine 101 (Molecular Probes) into the breast muscle 5-10 minutes before the final imaging session. This protocol yielded identical results compared with intramuscular injection of fluoresceine conjugated to 70,000 MW dextran (Molecular Probes) and labeled blood vessels for many (12+) hours. We then compared the blood vessel pattern to the migration trajectories of the GFP+ cells as well as the position of the soma to the nearest blood vessel.

Data Analysis and Statistics

Images were acquired using ScanImage software[34] and processed for contrast, color and alignment using ImageJ (NIH). Z-stacks from individual time points were aligned using the Stacks - shuffling/Align Slices plug-in available from the Wright Cell Imaging Facility. GFP+ cells were traced using Neurolucida (Microbright Field). To track migration paths image stacks acquired at different time points were first aligned in 3D using the position of the center of the cell body of DiI-labeled HVC_X neurons as reference points. The position of the center of GFP+ cells was identified by hand and recorded in imageJ. Migration trajectories were reconstructed using Matlab (Mathworks).

After processing we made two measurements of cell movement using the reconstructed trajectories. The first was path length (i.e. total distance we observed the cell to move) the second was displacement (i.e. radial distance, the distance between the start and end points along a path). Tortuosity (t) was calculated by dividing path length by displacement. In addition we also calculated displacement for subsets of the migration path corresponding to discrete time intervals (i.e. cell displacement over 3-hours), which we used to compare migration across different imaging timescales. T-test was performed using Matlab. The Rayleigh test[35] was performed in Matlab using a script written by Philip Berens (Max Planck Institute for Biological Cybernetics) and is available at http://www.mathworks.com/matlabcentral/fileexchange/10676.

Acknowledgements

We would like to thank Tim Gardner and Ni Ji for help with data collection, S. Turaga and A. Andalman for help with path reconstructions and T. Davidson for helpful comments on the paper.

REFERENCES

1. Altman, J. & Das, G.D. Autoradiographic and histological evidence of postnatal hippocampal neurogenesis in rats. *J Comp Neurol* **124**, 319-335 (1965).
2. Eriksson, P.S., *et al.* Neurogenesis in the adult human hippocampus. *Nat Med* **4**, 1313-1317 (1998).
3. Altman, J. Autoradiographic and histological studies of postnatal neurogenesis. IV. Cell proliferation and migration in the anterior forebrain, with special reference to persisting neurogenesis in the olfactory bulb. *J Comp Neurol* **137**, 433-457 (1969).
4. Curtis, M.A., *et al.* Human neuroblasts migrate to the olfactory bulb via a lateral ventricular extension. *Science* **315**, 1243-1249 (2007).

5. Kaslin, J., Ganz, J. & Brand, M. Proliferation, neurogenesis and regeneration in the non-mammalian vertebrate brain. *Philos Trans R Soc Lond B Biol Sci* **363**, 101-122 (2008).
6. Okano, H. & Sawamoto, K. Neural stem cells: involvement in adult neurogenesis and CNS repair. *Philos Trans R Soc Lond B Biol Sci* **363**, 2111-2122 (2008).
7. Paton, J.A. & Nottebohm, F.N. Neurons generated in the adult brain are recruited into functional circuits. *Science* **225**, 1046-1048 (1984).
8. Alvarez-Buylla, A., Theelen, M. & Nottebohm, F. Birth of projection neurons in the higher vocal center of the canary forebrain before, during, and after song learning. *Proc Natl Acad Sci U S A* **85**, 8722-8726 (1988).
9. Nordeen, K.W. & Nordeen, E.J. Projection neurons within a vocal motor pathway are born during song learning in zebra finches. *Nature* **334**, 149-151 (1988).
10. Kirn, J., O'Loughlin, B., Kasparian, S. & Nottebohm, F. Cell death and neuronal recruitment in the high vocal center of adult male canaries are temporally related to changes in song. *Proc Natl Acad Sci U S A* **91**, 7844-7848 (1994).
11. Kriegstein, A.R. & Noctor, S.C. Patterns of neuronal migration in the embryonic cortex. *Trends Neurosci* **27**, 392-399 (2004).
12. Lois, C., Garcia-Verdugo, J.M. & Alvarez-Buylla, A. Chain migration of neuronal precursors. *Science* **271**, 978-981 (1996).
13. Ayala, R., Shu, T. & Tsai, L.H. Trekking across the brain: the journey of neuronal migration. *Cell* **128**, 29-43 (2007).
14. Marin, O. & Rubenstein, J.L. A long, remarkable journey: tangential migration in the telencephalon. *Nat Rev Neurosci* **2**, 780-790 (2001).
15. Alvarez-Buylla, A., Theelen, M. & Nottebohm, F. Mapping of radial glia and of a new cell type in adult canary brain. *J Neurosci* **8**, 2707-2712 (1988).
16. Alvarez-Buylla, A. & Nottebohm, F. Migration of young neurons in adult avian brain. *Nature* **335**, 353-354 (1988).
17. Roe, T., Reynolds, T.C., Yu, G. & Brown, P.O. Integration of murine leukemia virus DNA depends on mitosis. *EMBO J* **12**, 2099-2108 (1993).
18. Kirn, J.R., Fishman, Y., Sasportas, K., Alvarez-Buylla, A. & Nottebohm, F. Fate of new neurons in adult canary high vocal center during the first 30 days after their formation. *J Comp Neurol* **411**, 487-494 (1999).
19. Barami, K., Iversen, K., Furneaux, H. & Goldman, S.A. Hu protein as an early marker of neuronal phenotypic differentiation by subependymal zone cells of the adult songbird forebrain. *J Neurobiol* **28**, 82-101 (1995).
20. Rakic, P. Mode of cell migration to the superficial layers of fetal monkey neocortex. *J Comp Neurol* **145**, 61-83 (1972).
21. Gleeson, J.G., Lin, P.T., Flanagan, L.A. & Walsh, C.A. Doublecortin is a microtubule-associated protein and is expressed widely by migrating neurons. *Neuron* **23**, 257-271 (1999).
22. Francis, F., *et al.* Doublecortin is a developmentally regulated, microtubule-associated protein expressed in migrating and differentiating neurons. *Neuron* **23**, 247-256 (1999).
23. Mullen, R.J., Buck, C.R. & Smith, A.M. NeuN, a neuronal specific nuclear protein in vertebrates. *Development* **116**, 201-211 (1992).

24. Bovetti, S., *et al.* Blood vessels form a scaffold for neuroblast migration in the adult olfactory bulb. *J Neurosci* **27**, 5976-5980 (2007).
25. Hatten, M.E. Riding the glial monorail: a common mechanism for glial-guided neuronal migration in different regions of the developing mammalian brain. *Trends Neurosci* **13**, 179-184 (1990).
26. Kakita, A. & Goldman, J.E. Patterns and dynamics of SVZ cell migration in the postnatal forebrain: monitoring living progenitors in slice preparations. *Neuron* **23**, 461-472 (1999).
27. Nadarajah, B., Alifragis, P., Wong, R.O. & Parnavelas, J.G. Neuronal migration in the developing cerebral cortex: observations based on real-time imaging. *Cereb Cortex* **13**, 607-611 (2003).
28. Tabata, H. & Nakajima, K. Multipolar migration: the third mode of radial neuronal migration in the developing cerebral cortex. *J Neurosci* **23**, 9996-10001 (2003).
29. Tanaka, D.H., *et al.* Random walk behavior of migrating cortical interneurons in the marginal zone: time-lapse analysis in flat-mount cortex. *J Neurosci* **29**, 1300-1311 (2009).
30. Wichterle, H., Garcia-Verdugo, J.M., Herrera, D.G. & Alvarez-Buylla, A. Young neurons from medial ganglionic eminence disperse in adult and embryonic brain. *Nat Neurosci* **2**, 461-466 (1999).
31. Moriyoshi, K., Richards, L.J., Akazawa, C., O'Leary, D.D. & Nakanishi, S. Labeling neural cells using adenoviral gene transfer of membrane-targeted GFP. *Neuron* **16**, 255-260 (1996).
32. Scott, B.B. & Lois, C. Developmental origin and identity of song system neurons born during vocal learning in songbirds. *J Comp Neurol* **502**, 202-214 (2007).
33. Lois, C., Hong, E.J., Pease, S., Brown, E.J. & Baltimore, D. Germline transmission and tissue-specific expression of transgenes delivered by lentiviral vectors. *Science* **295**, 868-872 (2002).
34. Pologruto, T.A., Sabatini, B.L. & Svoboda, K. ScanImage: flexible software for operating laser scanning microscopes. *Biomed Eng Online*, 2-13 (2003).
35. Fisher, N.I. *Statistical analysis of circular data* (Cambridge University Press, Cambridge [England] ; New York, 1995).

Figure 1 Migratory bipolar and complex cells in HVC.

a-b, Maximum intensity projection of GFP+ cells (green) in HVC and vimentin+ radial glia fibers (red) obtained from confocal microscopy on tissue sections. Bipolar cells, **a1**, appeared to migrate along radial fibers **a2**. Complex cells, **b1**, did not associate with radial fibers **b2**. Border between the ventricular zone (VZ) and brain parenchyma is indicated by a dotted white line. Scale bar is 50μm. **c**, Maximum intensity projection of a GFP+ migratory cell within HVC imaged *in vivo* using two-photon microscopy. HVC_X cell bodies are labeled with DiI (red). Scale bar is 25μm. **d**, Diagram of the labeling procedure used for two-photon microscopy. X-projecting HVC neurons (HVC_X, red dots) were retrogradely labeled by DiI injection into area X (red pointer). New neurons (green cell) were labeled by viral injection (green pointer) in the ventricular zone above HVC. Brain surface and skull are outlined in black. Scale bar is 2mm. **e**, Horizontal projection of the migratory trajectory of a GFP+ multi-polar cell in HVC imaged every 12 hours for 120 hours (black arrows). Red line indicates border of HVC. Scale bar is 100μm**. f**, Neuron morphology and position for trajectory shown in e. Time in hours is indicated in the upper left corner. Arrow indicates direction and distance of migration over the subsequent 12 hours. Scale bar is 50μm.

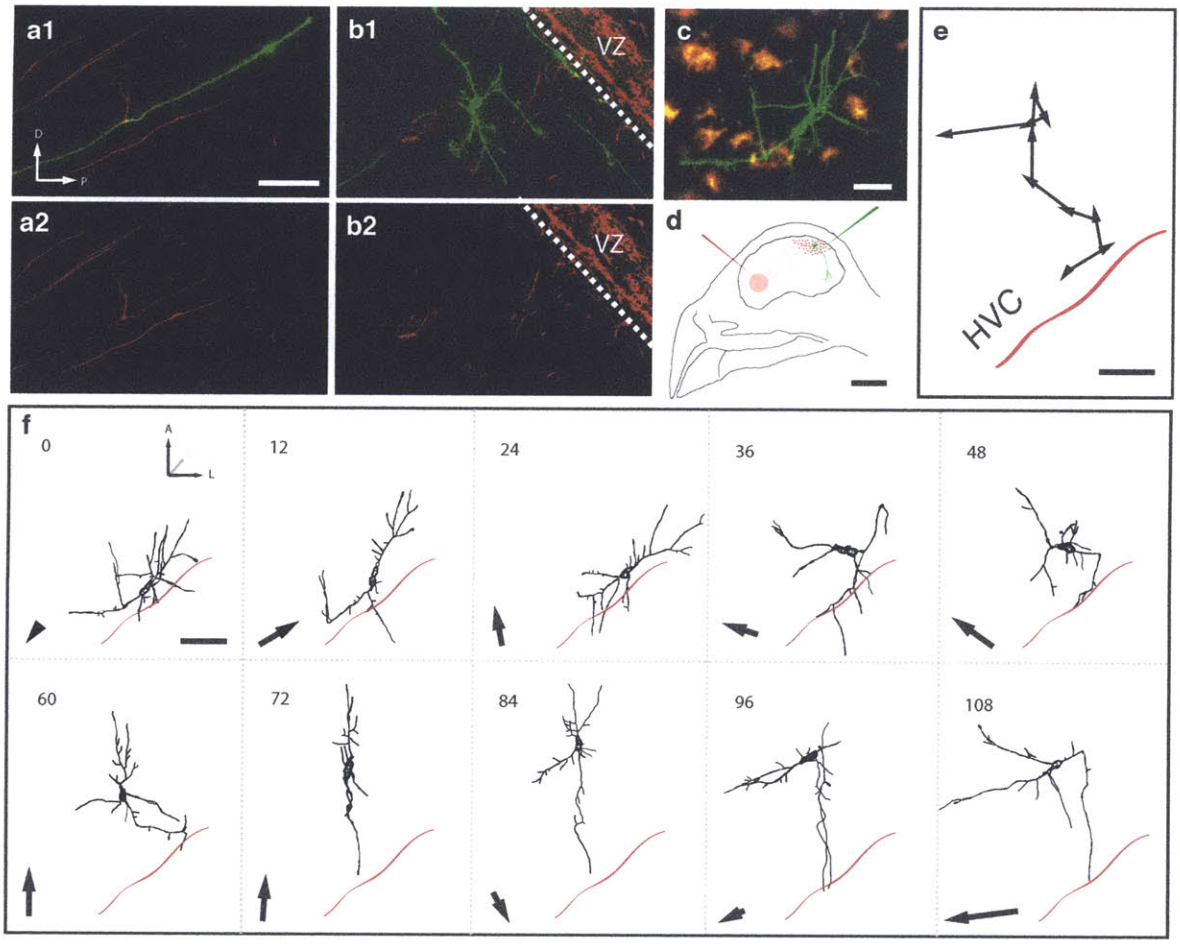
a1
b1
VZ
c
e
D
P
a2
b2
VZ
d
HVC
f
0
A
L
12
24
36
48
60
72
84
96
108

Figure 2 Soma translocation and direction changes in complex cell migration.

a-b Time-lapse maximal-projection *in* vivo two-photon images of HVC showing soma translocation and direction change in a migrating neuron. Time in minutes shown for each image. **a**, Detail of soma translocation between direction changes. Arrowheads at 0, 6, 30 and 36 min identify the soma during the stationary phase. **b**, Migrating multi-polar GFP+ complex cell (green) and surrounding DiI+ HVC_X cells (red). White dashed arrows at 0 min and 126 min indicate the upcoming direction of movement. Direction change at 126 min is accomplished by the movement of the cell body into a leading process first extended at -42 min (yellow arrowhead). Scale bar is 20 μm. **c-d**, Reconstruction of a 300-minute migratory trajectory in 3 dimensions (anterior/lateral/depth; A/L/Z). Black dots represent location of the soma center at 6-minute intervals in either A vs L coordinates (c) or L vs Z coordinates (d). Red line represents the smoothed trajectory (30-minute sliding average). Grey arrows, labeled T1 and T2, indicate turns in the migration trajectory. Scale bar 5μm. **e**. Plot of soma speed over time for trajectory shown in c & d. Raw data (red line) and 3-point sliding average (grey line) show speed calculated from smoothed trajectory in c & d. Turns T1 and T2 (grey arrows) occur during stationary phase.

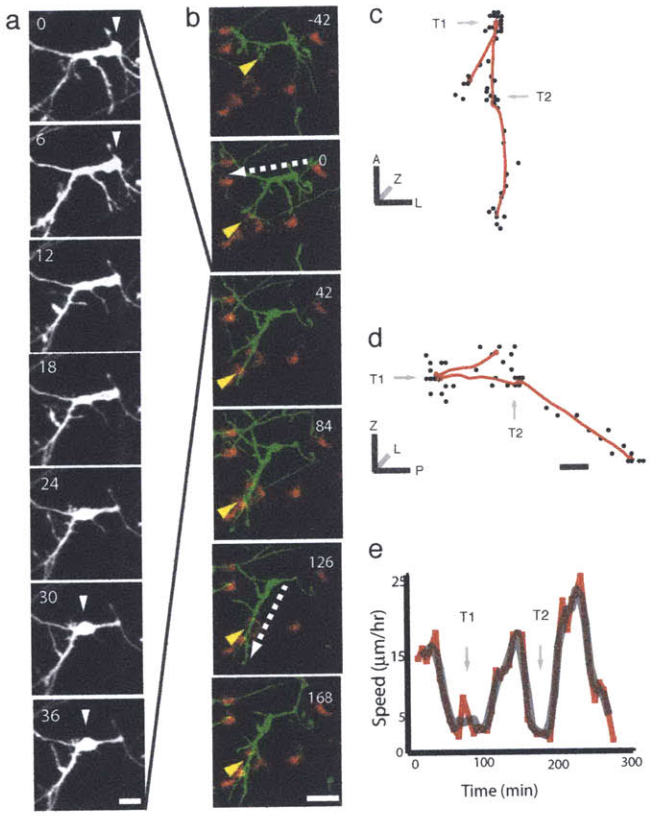
a
0
6
12
18
24
30
36
b
-42
0
42
84
126
168
c
T1
T2
A
Z
L
d
T1
T2
Z
L
P
e
Speed (µm/hr)
25
15
5
0
T1
T2
0
100
200
300
Time (min)

Figure 3 Dynamics of process growth *in vivo*

a, Imaging time series of a retracting process (red arrowhead at tip) and a growing process (yellow arrowhead at tip). Time in minutes indicated in each panel. Scale bar is 10μm. **b**, Histogram of rate of length changes in processes. Mean growth rate (-0.0215μm min^{-1}) for all processes was not significantly different from 0 (t-Test, Pval=0.625) suggesting that migratory cells did not grow in size, but merely changed shape. **c**, Processes within 60° of the direction of soma movement grew during the hour prior to movement of the cell body whereas processes oriented away from the direction of movement (>60°) retracted. Black dots are leading process, blue dots, non-leading process. Red line is 0μm growth. **d**, Single optical sections imaged with a confocal microscope of a GFP+ process tip (green) making contact (indicated by a white arrowhead) with a NeuN+ soma (red) in HVC. Each section is separated by a 1μm step, relative depth indicated on the upper right hand corner. Scale bar is 10μm.

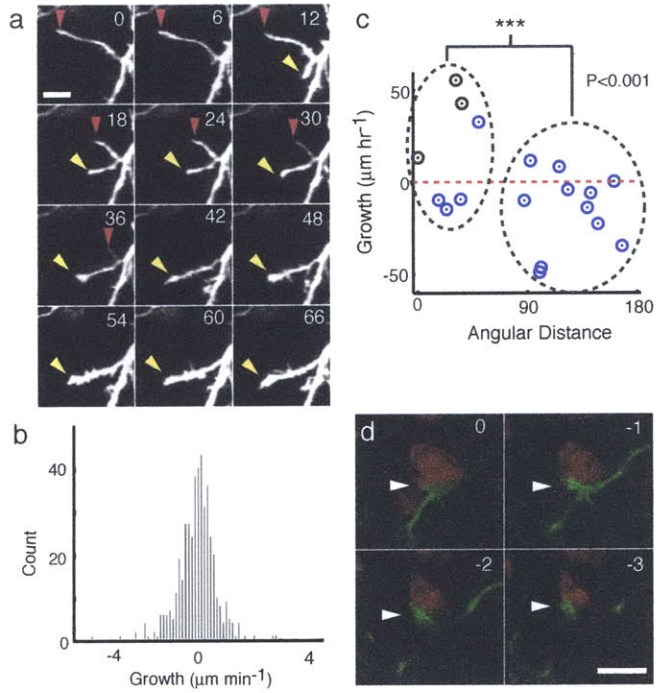
a
0
6
12
18
24
30
36
42
48
54
60
66
b
Count
40
20
0
-4
0
4
Growth (μm min-1)
c
***
P<0.001
Growth (μm hr-1)
50
0
-50
0
90
180
Angular Distance
d
0
-1
-2
-3

Supplemental

a-c, Immunohistochemistry against GFP and markers for neuronal fate. Left panels show a merge between GFP, shown in green and Dcx (**a**), Hu (**b**) or NeuN (**c**) shown in red. Right panels show the staining for the neuronal markers only. Arrow indicates the position of the GFP+ cell body. Scale bar = 10 μm. Inset in the lower right corner shows a high magnification image of the cell body. Scale bar = 10 μm. **d**, Horizontal projection of a migration path (white line) superimposed on a maximum projection image of sulforhodamine-labeled vasculature in HVC labeled (red). Scale bar is 25μm. **e**, Maximal intensity projection of a migratory cell in HVC and nearby blood vessels. Most (13/15) migrating cells did not make somatic contact with blood vessels. Mean distance from GFP+ soma to nearest blood vessel was 8.5μm. **f-g**, Heading of GFP+ cells in HVC. **f1**, Trajectories of 7 cells shown in the coronal plane. Each colored line represents the path of a single cell over 5.5 hours, aligned to begin at the origin. Scale bar = 5 μm. **g1**, Same trajectories in the horizontal plane. **f2-g2** Histogram of all directions taken by 21 GFP+ migrating cells. **f2**, Distribution of headings is biased away from the lateral ventricle in the coronal plane. **g2**, Distribution of headings is uniform in the horizontal plane.

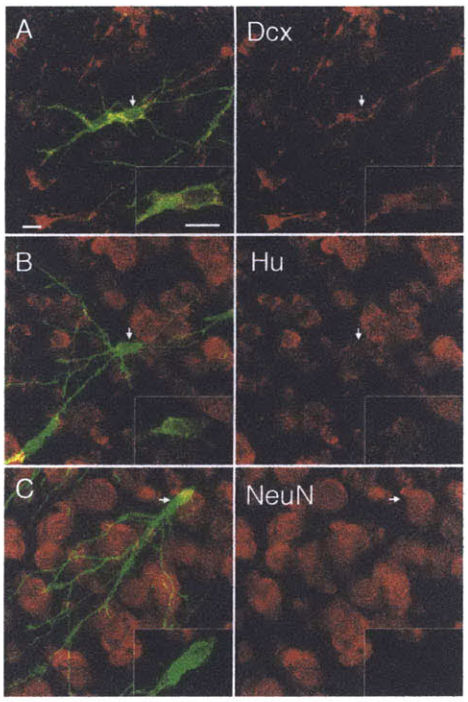
A
Dcx
B
Hu
C
NeuN

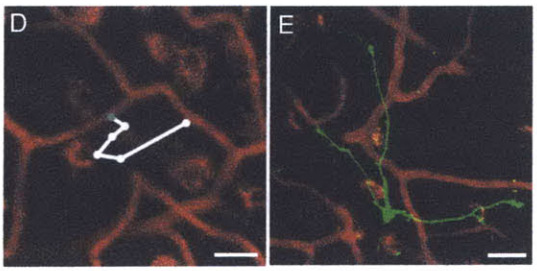
D
E

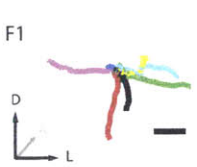
F1
D
L

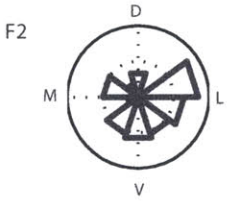
F2
D
M
L
V

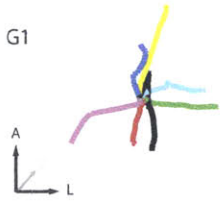
G1
A
L

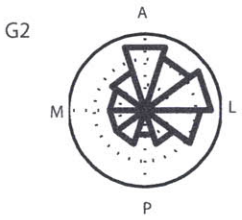
G2
A
M
L
P

Chapter 4

Discussion

In chapter 1, I proposed to study the addition of new neurons to the postnatal brain. I suggested that a useful approach to studying the biological function of postnatal neurogenesis is to directly observe this process. Chapters 2 and 3 describe the addition of new neurons to the High Vocal Center (HVC) in the juvenile male zebra finch during song learning. In these experiments we labeled newborn neurons with retroviruses, took many photos and speculated about the biology of these cells. We discovered where neuroblasts proliferate, how they move to their targets within the brain and what types of neurons they become.

In this final chapter I will present a model that attempts to integrate the results of the experiments described in the previous two chapters. I propose that the architecture of HVC emerges from a few basic rules about how new neurons behave during development as opposed to a detailed set of genetic instructions. Moreover, I suggest the possibility that stochastic cellular behavior plays an essential role in the development of the songbird brain and the brains of other animals. Finally I will discuss how our results impact current understanding of the evolution of song learning in birds.

We propose a model for the formation of HVC that supports the idea that the nervous system is a self-organizing system assembled by both genetically encoded instructions as well as random noise sculpted by selection. During vocal learning newborn neurons from the dorsal ventricular zone (VZ) migrate through the brain to their targets within HVC (Scott and Lois, 2007). These neurons initially travel along radial glia (Alvarez-Buylla and Nottebohm, 1988), but eventually detach and begin a search program (Chapter 3). The targets of this search appear to be the mature resident neurons in HVC. Our model is illustrated in figure 1.

New neurons seek out HVC_X neurons during the initial stages of HVC assembly. Since HVC_X neurons are born during embryogenesis, they arrive before the majority of HVC_{RA} neurons, which are born in the postnatal period. This observation suggests that HVC_X

neurons may play an important role in development and assembly of HVC. Indeed, cell type specific lesion experiments suggest that HVC_X neurons function primarily during song development. Specific deletion of HVC_X cells during adulthood has no effect on song, whereas deletion during learning disrupts normal singing (Scharff et al., 2000). A developmental role for HVC_X cells is further supported by the observation that exclusively these cells produce the trophic factor IGF-II (Holzenberger et al., 1997) and the differentiation factor retinoic acid (Denisenko-Nehrbass et al., 2000).

We observe that a newborn neurons stops migrating after it makes soma-soma contact with a HVC_X neuron. We anticipate that HVC_X cells provide the cue that triggers the cessation of movement in new neurons[1]. This cue may be electrical in nature, as has been proposed for neocortical interneurons (Bortone and Polleux, 2009), or chemical, as has been shown for neocortical projection neurons (D'Arcangelo et al., 1995). We have observed that new neurons do not stop at the first HVC_X neurons they make contact with, suggesting that not all HVC_X cells provide an effective stop signal. Instead we hypothesize that at any one time, a subset of HVC_X neurons express the stop signal and a migratory neuron may stop at anyone of these HVC_X cells. We anticipate that this subset is rather large fraction of HVC_X cells as the search time required to find a specific cells or a small number of cells would be too long to make this form of migration realistic. If there exist multiple possible HVC_X available for integration, search time would be decreased significantly. In this model the integration location of new neurons within HVC is not genetically determined. Instead, as with many complex patterns in biology, the precise architecture of HVC is the result of a combination of randomness acted on by selection.

1

Not all new neurons appear to stop at HVC_X, and as development process the percentage of new neurons that contact HVC_X declines. This observation suggests that as development proceeds mature HVC_{RA} neurons provide the stop signal. In juvenile zebra finches, 75% of new neurons contact HVC_X, whereas in adult canaries 50% of new neurons contact HVC_X and 25% contact HVC_{RA} (Kirn et al., 1999). In our experiments new neurons were labeled with retroviruses whereas the experiment in canaries, new neurons were labeled with BRDU. Therefore, the differences in percentages may be due to other factors.

The migratory behavior of new neurons results in the formation of neuronal clusters in HVC (Chapter 3, Kirn et al., 1999). Clusters are composed of the somata of multiple HVC_X, HVC_{RA} and interneurons that make tight soma-soma contact. This structure can be observed when both HVC_X and HVC_{RA} neurons are retrogradely labeled or when all neurons are stained, for instance with cresyl violet or antibodies against NeuN, a neuron specific antibody. From developmental evidence, we postulate that HVC_X neurons form the core of clusters. These neurons arrive before the addition of HVC_{RA} cells and appear to catalyze the formation of clusters by providing the stop signal to migrating newborn neurons (Chapter 3). We speculate that clusters, like columns in the cerebral cortex, may be anatomical and functional units essential to the learning and expression of neural sequences.

The functional consequence of these clusters is unknown. We hypothesize that a powerful electrical or chemical synapse exists between the cell bodies of mature neurons and the neighboring newborn neurons. Such a synapse, if strong enough, would cause the newborn neurons to fire near synchronously with the mature neuron. Synchrony could be used for the entrainment of newborn neurons into the existing circuit (see figure 2). In this model, a burst in a HVC_X neuron causes a spike in the adjacent new neuron. Inputs on the dendrites of the new neurons will be strengthened by Hebbian association when they fire contemporaneously with the burst of the mature neuron (Dan and Poo, 2004). Since the dendritic fields of mature HVC_X neurons and HVC_{RA} neurons are roughly the same diameter (Nixdorf et al., 1989), the inputs that drive the mature neuron to fire could be the same inputs that become strengthened on the new neuron. This mechanism would allow newborn neurons to acquire the firing time of neighboring mature neurons. Once these connections become sufficiently strong, the newborn neurons could become independent. Such a mechanism of entrainment might be essential to add new neurons to HVC without disrupting the pre-existing activity pattern so that song performance can be maintained in the face of an ever-changing cast of neurons.

Alternatively the new neurons could entrain the mature HVC_X cell. In the mammalian

cerebral cortex motor neurons extend axon collaterals toward the striatum (Ramón y Cajal, 1911) to provide an efference copy for learning. In the avian brain pallial motor neurons also send collaterals to the striatum, e.g. the LMAN axon splits *en route* to RA, sending a collateral to area X (Vates and Nottebohm, 1995) (Nixdorf-Bergweiler et al., 1995). HVC_{RA} cells do not extend an axon collateral to area X. However, if HVC_{RA} and HVC_X are strongly electrically coupled, HVC_X neuron's projection to area X may serve the same function as an axon collateral that reports the firing time of newly added HVC_{RA} cells to area X.

There exist two divergent strategies for the developmental origin of pattern in biological systems. The first posits that form is pre-specified by detailed genetic instructions. The second suggests that simple rules act upon randomly behaving cells to produce novel forms. Evidence exists for a role of both strategies during development, including the generation of brain architecture. The spatial patterns of simple morphological features in the nervous system, such as synapses, appear to be determined by trial and error (Meyer and Smith, 2006; Rankin and Cook, 1986). In contrast, a neuron's position in the brain and axon projection pattern are thought to be genetically determined and specified by the time of its last mitotic division and its birth place (Rakic, 1988). However, the observation that neurons are overproduced during development, has led to the hypothesis that entire neurons, like synapses, may integrate stochastically, and compete for survival (Buss et al., 2006).

Our data suggests that neuron position in the postnatal avian forebrain proceeds by selection acting on a biased random walk migration. The primary of evidence for this hypothesis is the cellular behavior of newborn neurons as they integrate into HVC. As described in chapter 3, the migratory neurons in HVC move in different directions independent of each other, make frequent turns and sometimes double-back on themselves. Their movements are well fit by a biased random walk model.

It is possible that these tortuous routes are required for movement through the mature brain, which has much less extracellular space then the developing brain (Bondareff and Narotzky, 1972). However, we also observed bipolar cells migrating through HVC migrate in straight lines, suggesting that extracellular space is not a fundamental constraint to all migration in the postnatal brain. Alternatively, an undiscovered scaffold, exhibiting the same geometric properties as the observed migration paths, guides new neurons final positions. However, the morphology of most newborn neurons in HVC is inconsistent with migration along a scaffold. Cells that migrate along scaffold exhibit a simple, linear morphology that reflects their commitment to a particular path (Hatten, 1990). The existence of multiple, dynamic, probe-like processes emanating from migratory neurons in HVC suggests that these cells are not guided by a particular scaffold. These processes contain swellings at their distal tip reminiscent of structures, such as the tip of leading process of a migrating neuron or axon growth cone, which perform sensory functions for cellular movement (Lambert de Rouvroit and Goffinet, 2001). The extension and retraction of these probe-like processes suggest that these neurons must find their path through a search-based mechanism.

One possible benefit of this strategy is that random cellular behavior can generate diversity from only a few simple rules. This strategy is used by the immune system for the generation of antibodies (Lederberg, 2002). This approach allows biological systems to produce complex patterns without the need to encode all the information in the genome. Just as it would require too much space in the genome to encode all possibly antibodies, it would require too much genome space to encode the exact positions of cells and synapses within the brain[2].

Over the course of evolution, traits can evolve to produce new forms. There is ample

---

[2] Self-organizing systems may also be more robust to mutation and variation. When governing rules are simple development may be more robust to noise and variations can accumulate with immediate selection.

evidence of this process at work in the formation of new morphological features (Carroll, 2008); however, little is know about how new behavioral traits evolve. Vocal learning is a striking example of behavioral specialization found in many avian species. Does this trait arise *de novo* or does it evolve from pre-existing neural circuitry and if so how? Indirect evidence has been found for both *de novo* evolution and homology to existing circuitry. Nuclei in the song system share a similar pattern of gene expression, which is distinct from surrounding tissue (Akutagawa and Konishi, 2001; George et al., 1995; Wada et al., 2004). Song nuclei are also highly interconnected with sparse connections to areas of the brain not involved in singing. These features led to the concept of the song circuit as a unique organ, distinct from the surrounding brain regions. This high degree of specialization combined with the molecular similarities between song nuclei might suggest a common developmental origin for brain regions that control singing.

Evidence from electrophysiology and immediate early gene expression suggests that song nuclei are homologous to surrounding brain regions (Feenders et al., 2008). These areas share similar projection patterns to the song nuclei, and are involved in similar behaviors, such as motor learning. The neuroanatomy of area X provides the most compelling evidence that the song system is homologous to an endogenous circuit for motor learning (Doupe et al., 2005; Person et al., 2008). Area X contains cellular elements, such as medium spiny neurons, that are highly conserved among the vertebrates and found in the surrounding avian striatum as well as the striatum of other species including mammals (Farries and Perkel, 2002).

In chapter 2 we examined the developmental origin of cells that join the song circuit. Developmental data can provide crucial insight into the evolutionary relationship between cell types. Our fate mapping experiments clearly demonstrate that neurons in area X and HVC originate from distinct populations of neural progenitors located in different portions of the VZ. Retroviral injections in the dorsal VZ produced labeled cells were observed both in HVC and in surrounding brain regions. We could also observe cells leaving HVC and entering the surrounding brain area. Retroviral injections into the ventral VZ produce labeled cells in area X and the surrounding striatum. These

results falsify the hypothesis for a common origin of all song nuclei and instead support the hypothesis that song nuclei are specializations of an endogenous circuit for motor learning.

More generally our data provides support for the idea that neuronal types are conserved across different species and different brain areas within the same species. In this model each neuronal type performs a specific computation within a neural circuit. The evolution of new behaviors can then result from new connections between neuronal cell types or the addition of new cell types into the neural circuit. In some cases new cell types may evolve. Cajal observed that the complexity of the neocortical neuropil increases from mice to primates, and hypothesized that an increase in the diversity of neuronal types could account the increased cognitive skills of higher vertebrates (Rakic, 1975).

New behaviors may also arise from the novel placement or connections of existing cell types. This model is difficult to distinguish from the creation of new kinds of neurons, since a satisfying criterion for the identification of neuronal types does not yet exist. The observation that some neurons can change morphology and physiology dramatically once they have differentiated suggests that morphology and projection pattern may not be suitable criteria for the judgment of cell types. For example, in cichlid fish, the neurons that produce gonadotrophin-releasing hormones can exhibit up to eight fold fluctuations in size depending on the animal's social environment (Francis et al., 1993) and neurons in the invertebrate nervous system can change their innervation targets during metamorphosis (Levine et al., 1995).

Direct observation of the cellular behavior has provided us with a number of testable hypotheses regarding the mechanism and regulation of brain assembly. The development of optical methods (Denk et al., 1990) and genetically encoded fluorescent markers (Cubitt et al., 1995) has allowed us to follow the behavior for single cells for long periods

of time in the intact animal. Our work, along with experiments of others using time-lapse imaging suggests that stochastic cellular behavior plays an essential role in the development of animals (Lichtman and Smith, 2008). How then do we move forward and test this model of brain development?

The rise of genetics and molecular biology during the 20th century has provided biologists with many tools to manipulate the behavior of cells. Direct observation and genetic manipulation are synergistic for the discovery of developmental mechanisms. The search for genes naturally biases research towards deterministic models of development, making stochastic behavior in biological systems more difficult to discover. Documenting cellular behavior allows us to formulate questions more precisely and to put genetic data into a logical framework. Quantitative characterization can provide both insight and constraint into the underlying mechanisms of cell behavior; however, molecular techniques are essential to test these hypotheses.

Due to songbirds' relatively long generation time (>100 days from egg laying to sexual maturity in the zebra finch), it is unlikely that classical forward genetics will be a successful approach to identifying genes in these species. An alternative approach to forward genetics is to use the existing genetic variation in a population to identify genes that control brain development or behavior. The songbirds are an excellent group for this approach. Their clade, the passeri, is extremely diverse - containing roughly 4000 species[3] - yet these species are highly similar with respect to morphology (Feduccia, 1996). Song learners (oscines) split from the non-learners (suboscines) during the cretaceous period (Ericson et al., 2002). However all oscines innately generate species-specific songs in the absence of learning. This innate song has diversified more recently. Sufficient genetic similarity exists for hybridization experiments to help dissect the genetic regulation of innate song features. Moreover the zebra finch genome is the second

---

[3] Different authors argue about the exact number, which ranges from 4177 to 4578 (roughly half of all bird species) (Feduccia, 1996). To put this number in context there are approximately 4300 mammalian, 6500 reptile and between 20,000 to 40,000 fish species (Tudge, 2000).

avian genome to have been sequenced. However, in order to make this project successful, tools to analyze the function of genes in the context of the intact organism will need to be developed. In the appendix, I describe the tools for the development of methods for the production of transgenic songbirds.

REFERENCES

Akutagawa, E., and Konishi, M. (2001). A monoclonal antibody specific to a song system nuclear antigen in estrildine finches. Neuron *31*, 545-556.
Alvarez-Buylla, A., and Nottebohm, F. (1988). Migration of young neurons in adult avian brain. Nature *335*, 353-354.
Bondareff, W., and Narotzky, R. (1972). Age changes in the neuronal microenvironment. Science *176*, 1135-1136.
Bortone, D., and Polleux, F. (2009). KCC2 expression promotes the termination of cortical interneuron migration in a voltage-sensitive calcium-dependent manner. Neuron *62*, 53-71.
Buss, R.R., Sun, W., and Oppenheim, R.W. (2006). Adaptive roles of programmed cell death during nervous system development. Annu Rev Neurosci *29*, 1-35.
Carroll, S.B. (2008). Evo-devo and an expanding evolutionary synthesis: a genetic theory of morphological evolution. Cell *134*, 25-36.
Cubitt, A.B., Heim, R., Adams, S.R., Boyd, A.E., Gross, L.A., and Tsien, R.Y. (1995). Understanding, improving and using green fluorescent proteins. Trends Biochem Sci *20*, 448-455.
D'Arcangelo, G., Miao, G.G., Chen, S.C., Soares, H.D., Morgan, J.I., and Curran, T. (1995). A protein related to extracellular matrix proteins deleted in the mouse mutant reeler. Nature *374*, 719-723.
Dan, Y., and Poo, M.M. (2004). Spike timing-dependent plasticity of neural circuits. Neuron *44*, 23-30.

Denisenko-Nehrbass, N.I., Jarvis, E., Scharff, C., Nottebohm, F., and Mello, C.V. (2000). Site-specific retinoic acid production in the brain of adult songbirds. Neuron *27*, 359-370.
Denk, W., Strickler, J.H., and Webb, W.W. (1990). Two-photon laser scanning fluorescence microscopy. Science *248*, 73-76.
Doupe, A.J., Perkel, D.J., Reiner, A., and Stern, E.A. (2005). Birdbrains could teach basal ganglia research a new song. Trends Neurosci *28*, 353-363.
Ericson, P.G., Christidis, L., Cooper, A., Irestedt, M., Jackson, J., Johansson, U.S., and Norman, J.A. (2002). A Gondwanan origin of passerine birds supported by DNA sequences of the endemic New Zealand wrens. Proc Biol Sci *269*, 235-241.
Farries, M.A., and Perkel, D.J. (2002). A telencephalic nucleus essential for song learning contains neurons with physiological characteristics of both striatum and globus pallidus. J Neurosci *22*, 3776-3787.
Feduccia, A. (1996). The origin and evolution of birds (New Haven: Yale University Press).
Feenders, G., Liedvogel, M., Rivas, M., Zapka, M., Horita, H., Hara, E., Wada, K., Mouritsen, H., and Jarvis, E.D. (2008). Molecular mapping of movement-associated areas in the avian brain: a motor theory for vocal learning origin. PLoS ONE *3*, e1768.
Francis, R.C., Soma, K., and Fernald, R.D. (1993). Social regulation of the brain-pituitary-gonadal axis. Proc Natl Acad Sci U S A *90*, 7794-7798.
George, J.M., Jin, H., Woods, W.S., and Clayton, D.F. (1995). Characterization of a novel protein regulated during the critical period for song learning in the zebra finch. Neuron *15*, 361-372.
Hatten, M.E. (1990). Riding the glial monorail: a common mechanism for glial-guided neuronal migration in different regions of the developing mammalian brain. Trends Neurosci *13*, 179-184.
Holzenberger, M., Jarvis, E.D., Chong, C., Grossman, M., Nottebohm, F., and Scharff, C. (1997). Selective expression of insulin-like growth factor II in the songbird brain. J Neurosci *17*, 6974-6987.
Kirn, J.R., Fishman, Y., Sasportas, K., Alvarez-Buylla, A., and Nottebohm, F. (1999). Fate of new neurons in adult canary high vocal center during the first 30 days after their formation. J Comp Neurol *411*, 487-494.
Lambert de Rouvroit, C., and Goffinet, A.M. (2001). Neuronal migration. Mech Dev *105*, 47-56.
Lederberg, J. (2002). Instructive selection and immunological theory. Immunol Rev *185*, 50-53.
Levine, R.B., Morton, D.B., and Restifo, L.L. (1995). Remodeling of the insect nervous system. Curr Opin Neurobiol *5*, 28-35.
Lichtman, J.W., and Smith, S.J. (2008). Seeing circuits assemble. Neuron *60*, 441-448.
Meyer, M.P., and Smith, S.J. (2006). Evidence from in vivo imaging that synaptogenesis guides the growth and branching of axonal arbors by two distinct mechanisms. J Neurosci *26*, 3604-3614.
Nixdorf, B.E., Davis, S.S., and DeVoogd, T.J. (1989). Morphology of Golgi-impregnated neurons in hyperstriatum ventralis, pars caudalis in adult male and female canaries. J Comp Neurol *284*, 337-349.
Nixdorf-Bergweiler, B.E., Lips, M.B., and Heinemann, U. (1995). Electrophysiological and morphological evidence for a new projection of LMAN-neurones towards area X.

Neuroreport *6*, 1729-1732.
Person, A.L., Gale, S.D., Farries, M.A., and Perkel, D.J. (2008). Organization of the songbird basal ganglia, including area X. J Comp Neurol *508*, 840-866.
Rakic, P. (1975). Local circuit neurons. Neurosci Res Program Bull *13*, 295-416.
Rakic, P. (1988). Specification of cerebral cortical areas. Science *241*, 170-176.
Ramón y Cajal, S. (1911). Histology of the nervous system of man and vertebrates (New York: Oxford University Press).
Rankin, E.C., and Cook, J.E. (1986). Topographic refinement of the regenerating retinotectal projection of the goldfish in standard laboratory conditions: a quantitative WGA-HRP study. Exp Brain Res *63*, 409-420.
Scharff, C., Kirn, J.R., Grossman, M., Macklis, J.D., and Nottebohm, F. (2000). Targeted neuronal death affects neuronal replacement and vocal behavior in adult songbirds. Neuron *25*, 481-492.
Scott, B.B., and Lois, C. (2007). Developmental origin and identity of song system neurons born during vocal learning in songbirds. J Comp Neurol *502*, 202-214.
Tudge, C. (2000). The variety of life : a survey and a celebration of all the creatures that have ever lived (London ; New York: Oxford University Press).
Vates, G.E., and Nottebohm, F. (1995). Feedback circuitry within a song-learning pathway. Proc Natl Acad Sci U S A *92*, 5139-5143.
Wada, K., Sakaguchi, H., Jarvis, E.D., and Hagiwara, M. (2004). Differential expression of glutamate receptors in avian neural pathways for learned vocalization. J Comp Neurol *476*, 44-64.

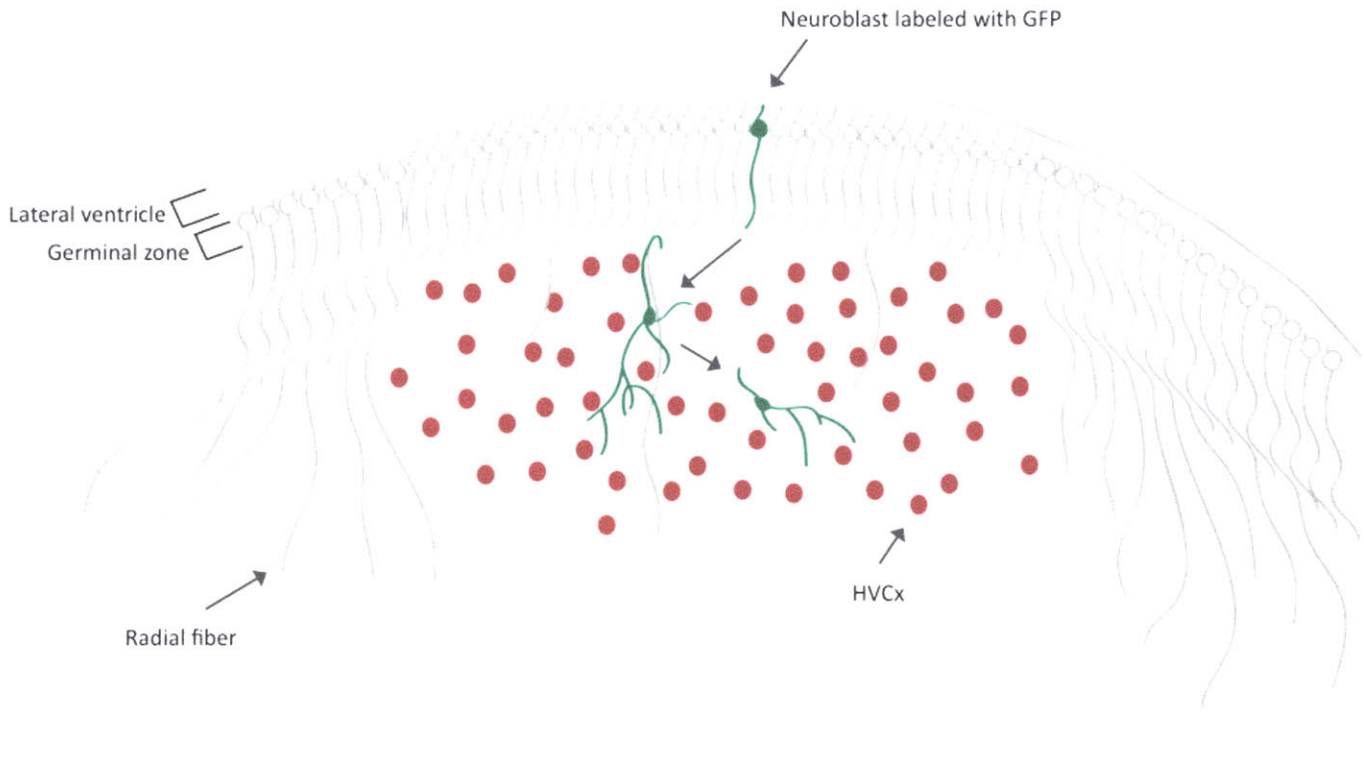

Figure 1. Model of migration of new neurons from the germinal zone into HVC.

This diagram shows a cross-sectional view of HVC and the adjacent ventricular zone. New neurons (labeled in green) are born in the germinal zone of the ventricular wall dorsal to HVC and can be labeled by an intracranial injection of a retroviral vector carrying the gene for GFP. After division, these cells migrate away from the lateral ventricle and enter HVC. Migrating neurons can either use the fibers of radial glia (labeled in grey) as guides or can migrate independent of scaffolds by a search mechanism. The targets of this search are the somata of mature HVC_X (red circles).

Figure 2. Model for the entrainment of new neurons into HVC

A. A newborn neuron (green) enters HVC and begins to search for the soma of a HVC_X neuron (red circles, labeled X1-X4). B. Once the newborn neuron contacts the soma of a HVC_X neuron (X3 in this case), the newborn cell stops migrating and begins to extend dendrites and receive synaptic input (black lines, labeled (t1-t4)). Synaptic inputs are assumed to be axons from a set of cells, where each set is active at a different time of the song. Each HVC_X neuron (X1-X4) also becomes active at a particular time in the song and we will assume that each HVC_X neuron receives input from synapses that fire contemporaneously. For instance t1 fires with X1, t2 fires with X2, etc. C. Strong electrical coupling between X3 and the new neuron causes the new neuron to fire contemporaneously with X3. Since t3 and X3 fire contemporaneously, the contacts between t3 and the new neuron become strengthened by hebbian association, whereas other inputs onto the new neuron are weakened. In this way newborn neurons come to be entrained to the firing times of mature neurons, a mechanism that may help maintain song performance in the face of postnatal neurogenesis.

A

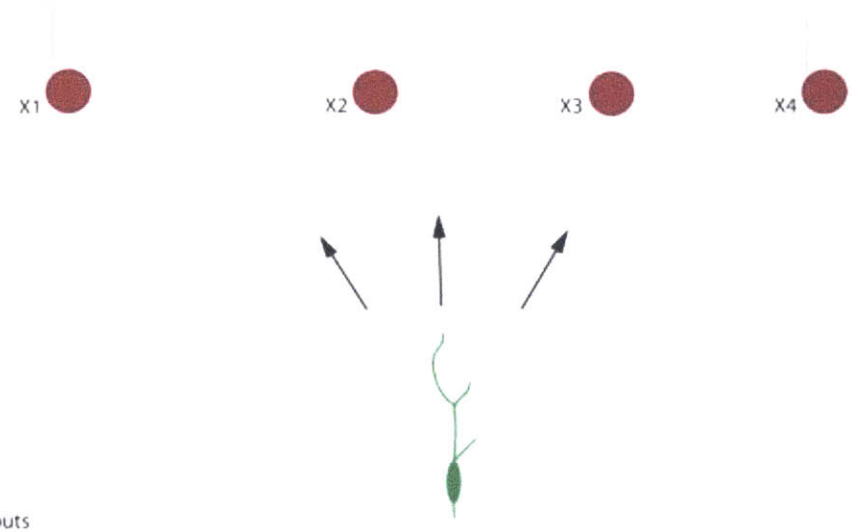
X1
X2
X3
X4

B

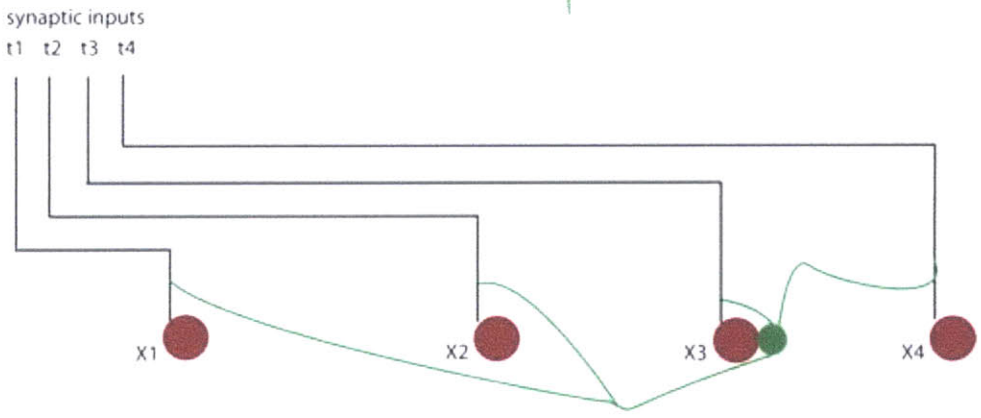
synaptic inputs
t1 t2 t3 t4
X1
X2
X3
X4

C

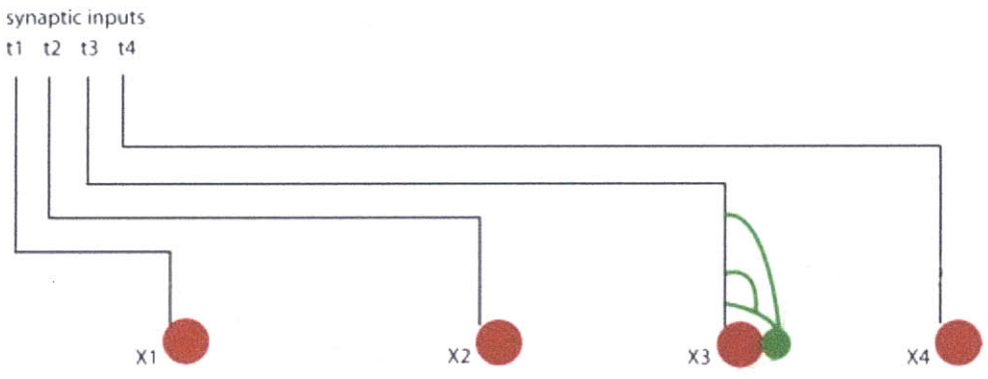
synaptic inputs
t1 t2 t3 t4
X1
X2
X3
X4

Appendix

Attributions.

This chapter was previously published as:

Scott, B.B., and Lois, C. (2005). Generation of tissue-specific transgenic birds with lentiviral vectors. Proceedings of the National Academy of Sciences. 102: 16443-7.

Generation of tissue-specific transgenic birds with lentiviral vectors

Benjamin B. Scott* and Carlos Lois

Picower Institute for Learning and Memory, Department of Brain and Cognitive Sciences, Massachusetts Institute of Technology, Cambridge, MA 02139

Communicated by Susumu Tonegawa, Massachusetts Institute of Technology, Cambridge, MA, September 27, 2005 (received for review January 12, 2005)

Birds are of great interest for a variety of research purposes, and effective methods for manipulating the avian genome would greatly accelerate progress in fields that rely on birds as model systems for biological research, such as developmental biology and behavioral neurobiology. Here, we describe a simple and effective method for producing transgenic birds. We used lentiviral vectors to produce transgenic quails that express GFP driven by the human synapsin gene I promoter. Expression of GFP was specific to neurons and consistent across multiple generations. Expression was sufficient to allow visualization of individual axons and dendrites of neurons *in vivo* by intrinsic GFP fluorescence. Tissue-specific transgene expression at high levels provides a powerful tool for biological research and opens new avenues for genetic manipulation in birds.

avian | genetics | lentivirus | synapsin | neuron

Transgenesis has proven to be one of the most powerful tools for modern biology (1). Genetic experiments using transgenic mice, fish, worms, and flies have revolutionized the study of developmental biology, neurobiology, and immunology, among other fields. Unfortunately, transgenic tools remain unavailable for many popular research species. In particular, useful transgenic birds have been difficult to produce, although numerous attempts have been made for >25 years (2).

One major obstacle to genetic manipulation in birds has been achieving reliable expression of the transgene. Foreign DNA can be efficiently introduced into avian genomes by infecting the early embryo with oncoretroviral vectors (3). A number of groups have successfully produced transgenic chickens using this general method (4, 5, 6). However, in transgenic birds produced by using oncoretroviral vectors, transgene mRNA and protein product are present at low or undetectable levels, possibly due to developmental silencing (6).

Another class of retroviruses, the lentiviruses, is not silenced during embryonic development. Transgenic mice and rats generated by using lentiviral vector show reliable transgene expression (7). Lentiviral vectors have also been used to generate transgenic pigs and cattle (8, 9), and, in principle, they should allow for the generation of transgenic birds. Indeed, promising results were obtained in chickens with the use of recombinant equine infectious anemia virus (EIAV), a type of lentivirus (10). Transgenic chickens were generated that expressed GFP in some tissues; however, the pattern of GFP expression was inconsistent with the expected activity of the viral promoter used. Recently, another study reported the use of HIV-1-based lentiviral vectors to generate transgenic chickens that ubiquitously express GFP under the control of the phosphoglycerol kinase (PGK) promoter (11). Interestingly, the frequency of germ-line transmission among chicken founders reported in this study was <1%, whereas the rate of transgenesis in mice is ≈80% (7). These reports demonstrate the potential strengths of lentiviral vector-based avian transgenesis. However, to be useful, both of the following should apply: a system for the production of transgenic birds should be efficient and gene expression should be predictable and reliably controlled by the regulatory sequences of the transgene.

Here, we describe the efficient generation of transgenic birds with neuron-specific expression using lentiviral vectors derived from HIV-1. Vectors derived from HIV-1 have been shown to allow faithful tissue-specific expression in transgenic mice (7). To test whether lentiviral vectors could be used to direct transgene expression specifically in neurons, we used the promoter sequence from the human synapsin I gene (Hsyn). Lentiviral vectors engineered to contain Hsyn driving GFP were introduced into Japanese quail embryos. This method produced mosaic founder quails that expressed GFP in neurons and transmitted the transgene to their progeny, which expressed high levels of GFP selectively in neurons. In transgenic animals, the axons and dendrites of developing neurons were easily detectable by fluorescence microscopy.

Our technique can be modified for use in other avian species and can be used to alter the expression of endogenous genes. Birds are important model organisms for many problems in biology but are not more widely used because effective methods for genetic manipulation in these animals do not exist. Lentiviral transgenesis is a versatile and powerful tool that will provide a molecular approach to studying biological questions in birds and will make possible new avenues for research in a group of popular research animals for which modern genetic techniques were previously unavailable.

Methods

Construction of Lentiviral Vectors. We have developed a vector for neuron-specific transgene expression based on FUGW, a self-inactivating lentiviral vector derived from the HIV-1 (7). We replaced the ubiquitin-C promoter region of FUGW with a regulatory sequence that lies −570 to −93 bp from the transcription start site of the Hsyn. The resulting construct is called HsynGW (Fig. 1). Recombinant HsynGW virus was prepared and stored as described (7). We titrated the virus on primary cultures from newborn rat cortex and confirmed that GFP expression *in vitro* was specific to neurons.

Production of Mosaic and Transgenic Quails. Freshly laid Japanese quail (*Coturnix coturnix japonica*) eggs were purchased from CBT Farms (Chestertown, MD) and arrived the next morning by express courier. Eggs were placed on their sides for 1 h before injection to allow the embryo to float to the top of the yolk. Before windowing, egg shells were disinfected with 70% ethanol. To gain access to the embryo, a 4-by-4-mm window was drilled at the top of the eggshell with a handheld rotary tool (Dremel, Mount Prospect, IL), and the shell membrane was removed with forceps. Viral vector solution of HsynGW (10^7 infectious particles per microliter) was loaded into a pulled glass capillary (Sutter Instruments, Novato, CA; o.d. = 1 mm, i.d. = 0.75 mm) with a tip that had been scored with a ceramic tile (Sutter) and

Conflict of interest statement: No conflicts declared.

Freely available online through the PNAS open access option.

Abbreviation: Hsyn, human synapsin I gene.

*To whom correspondence should be addressed. E-mail: bbscott@mit.edu.

© 2005 by The National Academy of Sciences of the USA

NEUROSCIENCE

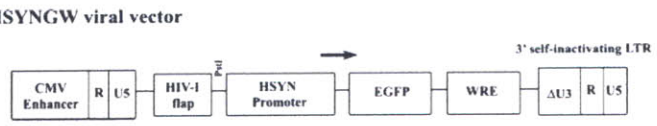

Fig. 1. Diagram of the relevant regions of the HsynGW vector used to generate mosaic quails. The 5′ CMV enhancer is used to express genomic viral RNA during the production of vector particles but is excluded from the integrated proviral DNA in the bird's genome. The position of the restriction site PstI used for Southern blot analysis of proviral integration is indicated. The arrow located on top of the HSyn promoter box marks the start site of transcription of EGFP. The woodchuck hepatitis virus posttranscriptional regulatory element (WRE) was included to increase the level of EGFP transcription. The U3 region of the viral 3′ LTR (ΔU3) contains a deletion that minimizes the endogenous transcriptional activity of the LTRs of the integrated provirus.

broken flush to 20 μm o.d. Embryos were observed with a dissecting microscope at $\times$16 magnification, and 3 μl of vector solution was injected into the subgerminal cavity below the embryo with an oil hydraulic injection system (CellTram oil, Eppendorf). To allow visualization of the injection site, 5% phenol red in PBS was added to the viral solution. Injections were considered successful if the viral solution spread horizontally in a circle below the embryo and if the perimeter of the viral solution reached the borders of the area opaca (for a useful atlas of avian embryo anatomy, see Bellairs and Osmond, ref. 12). More than 90% of injections were successful according to these criteria. After a successful injection, eggs were sealed to prevent microbial contamination and fluid loss during incubation.

To seal the eggshell, a round glass coverslip was placed over the shell window and was attached to the egg with a biocompatible silicone elastomer (Kwik-Cast, WPI Instruments, Waltham, MA). Eggs were placed blunt end up into a forced air incubator (Brinsea, Titusville, FL), with a temperature of 38°C and a relative humidity of 45% until hatching, and were turned periodically. Eggs hatched after 18 days of incubation and were subsequently kept in a heated brooder. Three weeks later, founder mosaic quails were placed in a cage until they reached sexual maturity at $\approx$7 weeks, at which time they were mated to wild-type quails. Eggs from transgenic founders were collected, placed in the incubator, and examined at different stages of development. Embryos were examined both with epifluorescent and confocal microscopes. To genotype hatchlings, we nicked the alar vein on the wing of 5-day-old animals and collected 70 μl of blood.

Analysis of Transgene Copy Number and Expression Profile. Genomic DNA from blood was extracted from whole blood samples by overnight digestion in proteinase K followed by phenol chloroform extraction (13). DNA was digested with the restriction enzyme PstI overnight at 37°C. PstI cuts once inside the integrated provirus between the 5′ viral LTR and the Hsyn promoter (Fig. 1). Southern blot hybridization was performed with a ^{32}P-labeled DNA probe against the GFP sequence.

To examine GFP expression, juvenile and adult quail were transcardially perfused with 3% paraformaldehyde in PBS. Brains were cut into 50-μm sections on a vibrating microtome. Sections were counterstained with Hoechst 33258 (Sigma–Aldrich; 1.2 μg/ml) for 5 min at room temperature, mounted in 50% glycerol, and examined under epifluorescence or with a confocal fluorescent microscope. To examine whether GFP expression was confined to neurons, we performed double immunocytochemistry by incubating sections overnight at 4°C with a Rabbit polyclonal anti-GFP antibody (Abcam, Cambridge, MA; dilution 1:1,000) and mouse monoclonal anti-NeuN (Chemicon; dilution 1:500). Both antibodies were diluted in a blocking solution containing 0.1% Triton X-100 and 10% normal goat serum. The next day, sections were washed with PBS

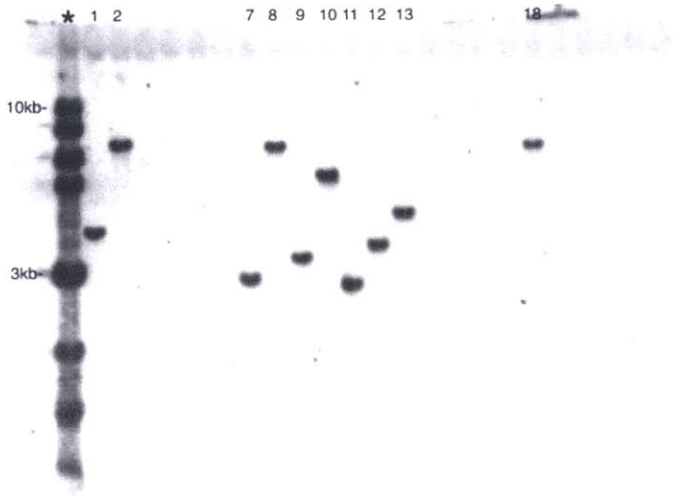

Fig. 2. Transgenic animals carry single copies of the HsynGW provirus. Southern blot analysis of genomic DNA from 23 progeny of Hsyn mosaic founders. *, Lane with molecular weight standards (1-kb ladder, New England Biolabs). All other lanes contain genomic DNA from individual F_1 quails. Genomic DNA extracted from quail blood or embryos was digested with the restriction enzyme PstI, which cuts once inside the lentiviral vector. The probe used hybridizes to a 500-bp section of GFP. Transgenic birds were found to carry only single copies of the integrated provirus as indicated by the presence of a single band per lane on the Southern blot (lanes 1, 2, 7–13, and 18).

three times for 1 h each and incubated with a fluorescein-conjugated anti-rabbit secondary antibody (Fl-1000, Vector Laboratories) and a Texas red-conjugated anti-mouse antibody (Ti-2000, Vector Laboratories) at room temperature for 1 h in blocking solution. Finally, sections were washed with PBS three times for 1 h each, mounted in 50% glycerol, and examined under epifluorescence or with a confocal fluorescent microscope.

Results

Production of Mosaic Quails and Germ-Line Transmission of the Transgene. Mosaic quails were produced by infecting the blastodiscs of unincubated eggs with concentrated HsynGW lentiviral vector. At this stage, the quail blastodisc is a thin sheet consisting roughly of 40,000 cells. We infected 80 embryos with this method, and, of these, 8 hatched and developed to adulthood. Because the vector particles are too large to diffuse throughout all layers of the blastodisc, this method infects only a percentage of the cells of the embryo. Therefore, it is expected that these founder quails will be mosaic for the presence of the transgene. Accordingly, we expected only a percentage of the somatic tissue of each quail to carry the transgene. To examine the expression of the transgene in mosaic founders, we observed tissue sections from two adult quails (>50 days old).

In mosaic animals, GFP expression was confined to the peripheral and central nervous system. In tissue sections from the brain, we could observe GFP expression in the cell bodies of neurons, axons, and dendrites. In particular, the dendritic fan and soma of Purkinje cells of the cerebellum and the axons of projection cells in the hippocampus were brightly fluorescent. The neurons of the forebrain and optic tectum were also well labeled. Although individual cell bodies were easily distinguished, the high density of labeled neurons made it difficult to identify the processes of individual neurons. As expected, only a percentage ($\approx$10%) of neurons in the mosaic founders were GFP-positive (data not shown).

To examine the transmission rate of the transgene to the progeny, we bred six adult founder (F_0) mosaics to wild-type quails. The progeny of F_0 mosaics were screened by Southern

Table 1. Germ-line transmission rates in mosaic and transgenic quails

Generation/ sex	No. of progeny examined	No. of progeny carrying transgene	No. of progeny expressing GFP	Germ-line transmission frequency, %
F_0/M	16	5	5	31
F_0/M	47	8	7*	17
F_0/M	12	1	1	8
F_0/M	35	0	0	
F_0/F	12	4	4	33
F_0/F	4	1	1	25
F_1/M	17	10	10	59
F_1/M	8	5	5	62

M, male; F, female; F_0, mosaic founder; F_1, first generation transgenic.
*In one transgenic embryo GFP expression was not observed.

blot analysis to test for the presence of the transgene (Fig. 2). Germ-line transmission rate ranged between 8% and 33%, depending on the founder (results are summarized in Table 1). One founder mosaic did not produce any transgenic offspring. Of the 16 transgenic offspring found, each carried a single copy of the transgene (as assessed by Southern blotting).

Expression Pattern in F_1 and F_2 Transgenics. GFP expression was first visible in transgenic embryos after 60 h of incubation. At this time, GFP was visible in the soma of cells in the rostral spinal cord and forebrain. GFP expression increased steadily through early development. By 72 h of incubation, GFP fluorescence was present in the axon and dendrites of cells in the brain and spinal cord. After 4 days of incubation, individual neurons in the forebrain of could be identified (see Fig. 4 *A* and *B*). Confocal microscopy performed on the intact living embryo at this stage revealed the axons and cell bodies of single neurons of the forebrain (Fig. 4*B*). By embryonic day 6, the brain, spinal cord, and peripheral nervous system showed strong GFP expression (Fig. 3). The innervation of the limb buds was visible both in the intact live embryo (Fig. 3*A*) and in tissue sections (Fig. 3*D*). The eyes of the transgenic embryos were particularly well labeled with GFP (Fig. 4 *C* and *D*). GFP expression in the retina was visible through the pupil. In addition, axons innervating the iris and cornea could be imaged easily in the live embryo (Fig. 4 *C* and *D*). The observed temporal expression pattern of GFP in the transgenic quails is similar to that of the endogenous synapsin gene I in chicken embryos (14).

The level of GFP expression was comparable in 15 of 16 F_1 transgenics. However, one embryo that carried a transgene copy as assessed by Southern blot analysis did not display any detectable GFP expression. A positional effect may have been responsible for the lack of expression in this animal, because the site of transgene integration on a chromosome can exhibit strong effects on transgene transcription (15).

Two transgenic quails (F_1) carrying different insertions were allowed to develop to sexual maturity. These quails were mated with wild-type quails to determine whether GFP expression levels and tissue specificity were consistent across multiple generations. Progeny were screened by Southern blot analysis to test for the presence of the transgene, and by fluorescence microscopy to check for GFP expression. The transgene was transmitted to F_2 progeny at ratios that approached those expected from the Mendelian inheritance of individual alleles: 59% (n = 17) and 62% (n = 8) for each parent, respectively. Examination of embryonic, juvenile, and adult quails revealed comparable spatial and temporal GFP expression pattern in F_1 and F_2 transgenics.

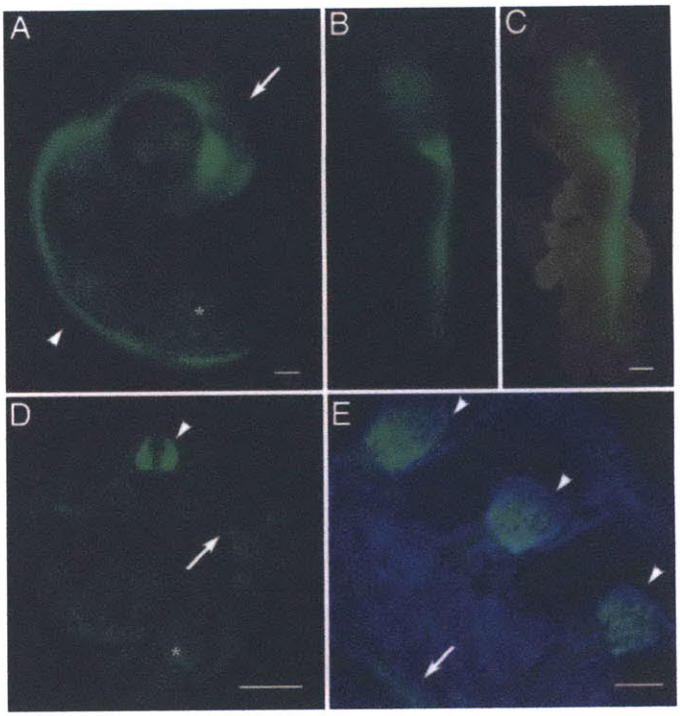

Fig. 3. GFP expression in an embryonic day 6 transgenic quail. (*A*) Profile view of GFP expression in an intact embryo. Arrow indicates head; arrowhead indicates spinal cord. GFP fluorescence in the retina can be seen through the pupil. At this stage, the sensory and motor innervation of the developing limb buds begins to be visible (*). (*B*) GFP fluorescence in the brain and spinal cord. (*C*) Merged view of fluorescence and bright field of the same embryo shown in *B*. (*D*) Cross-sectional view at the level of the forelimbs. Arrowhead indicates the spinal cord. Arrow indicates a bundle of motoneuron axons innervating the developing limb bud. The signal observed in the embryo's ventral surface (*) is due to autofluorescent signal originating from the skin. (*E*) Sagittal section of three spinal ganglia (arrowheads). A short section of the spinal cord labeled by GFP occupies the bottom left of the panel (arrow). Neurons are labeled by intrinsic GFP fluorescence (green), and nuclei of all cells are labeled by Hoechst 33258 (blue). (Scale bars: *A*, *C*, and *D*, 1 mm; *E*, 100 μm.)

Tissue specificity in both F_1 and F_2 generations was examined in whole-mount sections from day 6 embryos and in tissue sections from the brains of juvenile and adult quails. GFP-positive neurons were clearly visible throughout the brain, spinal cord, and peripheral nervous system of transgenic animals, but not in controls. Sections from the cerebral hemispheres, cerebellum, and optic tectum were processed for immunohistochemistry with antibodies against GFP and NeuN, a nuclear protein specific for many types of mature neurons (16). No GFP-positive cells were observed outside the central or peripheral nervous system. NeuN was observed in the cell nuclei and perinuclear cytoplasm of cells in the forebrain, cerebellum, and optic tectum. All NeuN-positive cells expressed GFP, and most GFP-positive cells were also labeled by NeuN (Fig. 5 *A–C*). Some cells, such as Purkinje neurons of the cerebellum, were GFP-positive, but not NeuN-positive (Fig. 5*D*). This result was expected because some cell types, including Purkinje neurons, are not well labeled by the NeuN antibody (16). However, wherever GFP-positive cells were not also labeled with NeuN, cell morphology clearly indicated that these GFP-labeled cells were neurons. The observation that GFP-expressing cells always had a neuronal morphology, were labeled with the neuN antibody, and were restricted to the nervous system demonstrates that transgene expression was specific to neurons.

Discussion

In this study, we have demonstrated that lentiviral vectors can be used to efficiently produce transgenic quails that express

NEUROSCIENCE

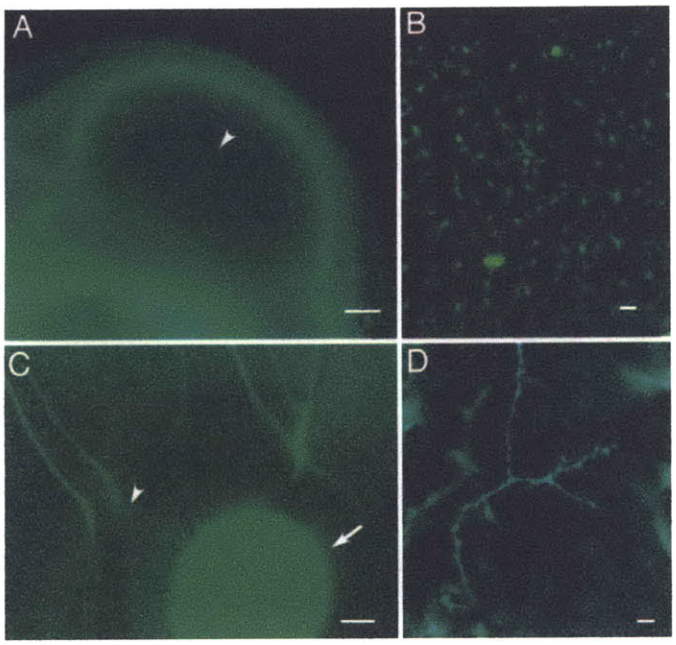

Fig. 4. Imaging of GFP-expressing neurons in live embryos. (*A*) GFP-expressing neurons in the brain of embryonic day 4 transgenic quail at low magnification. Arrowhead indicates region magnified in *B*. (*B*) Cell bodies and axons of GFP-labeled neurons in a live embryo, viewed by confocal microscopy. (*C*) Eye of live embryonic day 6 quail. Arrow indicates GFP-positive retina viewed through the pupil. Arrowhead indicates axons innervating the cornea and iris. (*D*) Individual axon innervating the cornea, viewed by confocal microscopy. (Scale bars: *A* and *C*, 250 μm; *B* and *D*, 10 μm.)

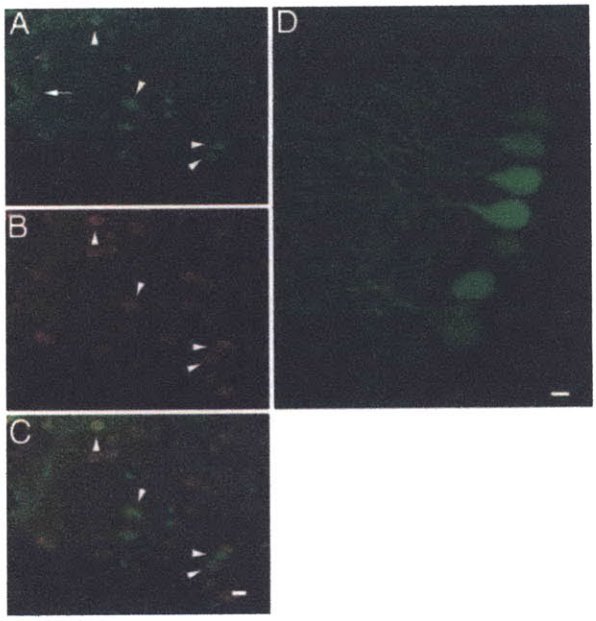

Fig. 5. Selective expression of GFP in neurons from HsynGFP transgenic quails. Shown is immunohistochemistry against GFP (*A*) and neuron-specific marker NeuN (*B*) in sections from the forebrain of transgenic quails. (*C*) A merged image of *A* and *B*. Immunohistochemistry was performed against GFP because intrinsic GFP fluorescence fades after fixation. Tissue sections were viewed with a confocal microscope. (*B*) NeuN staining was observed in the nuclei and perinuclear cytoplasm of neurons. Neuron processes were labeled only by GFP (see arrow in *A*). In most cases, GFP-positive cell bodies were also NeuN-positive (exemplary cells are marked by arrowheads in *A*, *B*, and *C*). Some cells with neuron morphology (i.e., bearing axons and dendritic arbors), such as the Purkinje cells of the cerebellum (*D*), were GFP-positive, but not NeuN-positive. This result was expected because previous works have shown that NeuN antibodies do not label all neurons. (Scale bar: 10 μm.)

GFP at high levels. Importantly, the transgene was expressed selectively in neurons, a pattern we expected based on the transcriptional activity of the synapsin promoter that we engineered into our vector. Achieving the reliable spatial and temporal expression pattern of a transgene is a critical step in the development of transgenic technologies in birds. Our vector contains two elements that we expect to contribute to the faithful expression of GFP in neurons: a highly conserved promoter and a recombinant viral backbone engineered not to interfere with transgene expression.

For our promoter, we chose a region of the transcriptional regulatory element of the Hsyn, an element known to produce neuron-specific expression *in vitro* (17, 18). Although the avian synapsin homolog has not been sequenced, the promoter region for the synapsin I gene is highly conserved in several mammalian species (19). In another study (11), the promoter region for phosphoglycerol kinase was used to direct ubiquitous expression in transgenic chickens. In contrast, previous studies with transgenic birds have often relied on viral promoters such as the SV40 promoter (4) and the CMV promoter (5). It is difficult to predict the expression pattern of these promoters because they show no similarity to any known endogenous promoter in birds. When a lentiviral vector carrying the CMV promoter was used to produce transgenic chickens, transgene expression was primarily in the pancreas and to a lesser extent in the liver, skin, muscle, and lining of the intestine (10). In addition, the level of transgene expression in these tissues was variable between different transgenic lines.

In addition to the promoter used, the viral backbone can also affect transgene expression. Viral sequences of retroviral-based vectors have been shown to affect gene expression in two ways. (*i*) Oncoretroviral elements and associated sequences are silenced during development by *de novo* methylation of cytosine residues. Methylation stimulates the formation of heterochromatin, which blocks the transcriptional activity of the region surrounding the integrated retrovirus, and ultimately results in low or undetectable levels of transgene expression. This effect had been clearly documented in mice (20), and there is evidence suggesting this effect may also occur in birds (6). (*ii*) Retroviral LTRs contain internal promoters and enhancers, which may interfere with the expression of the transgene in both oncoretroviral and lentiviral based vectors. The vector used in our study has been engineered to minimize the transcriptional activity of the LTRs (21), and it was shown to faithfully allow tissue-specific transgene expression without developmental silencing (7). Thus, recombinant HIV-derived lentiviral vectors are an effective vector to allow tissue-specific expression in both transgenic mammals and birds.

We chose quails as a bird model for transgenesis because of their widespread use in developmental studies and for a number of practical reasons (22). Quails are excellent breeders, require less space to house than chickens, and develop rapidly. Incubation lasts 18 days, and hatchlings become sexually mature after 7 weeks. Eggs are easy to obtain from farms by mail so it is not necessary to maintain a breeding colony solely to produce eggs for the generation of mosaics. Transgenics of other avian species would require more time and space to breed. Because the organization of the avian embryo is well conserved at the time of oviposition, we do not anticipate any major obstacles to the generation of transgenics in other species, as suggested by previous experiments in chickens (10, 11).

Transgenesis with lentiviral vectors will allow for the molecular dissection of physiological processes in birds with a level of precision unattainable with other methods. Lentiviral transgenesis can be used to interfere with normal gene expression in a

number of ways. (*i*) Genes of interest can be ectopically expressed to modify the development or function of cells. (*ii*) Dominant-negative constructs can be introduced to block normal gene function (23). (*iii*) Lentiviral vectors carrying short interfering RNAs (siRNAs) can down-regulate endogenous mRNAs and can be used against genes for which no dominant negative constructs are known (24). These powerful manipulations make lentiviral transgenesis a useful genetic tool to study complex biological processes in birds.

For our initial experiments we chose a marker that enables the visualization of individual neurons in the developing embryo. Using the Hysn promoter to drive expression of GFP in the neurons of quails, we were able to label individual cells beginning 60 h after incubation. By 72 h, GFP had diffused into and labeled the dendrites and axons of neurons in the forebrain and spinal cord. Because their neurons are well labeled and because of the early age at which GFP expression begins, these birds will be useful for *in vivo* imaging studies of neural development. Strains of transgenic mice with neuron-specific GFP expression have been valuable for *in vivo* studies of synaptogenesis and neuromuscular junction development (25). However, imaging mouse pups during embryonic development is difficult because the mother must be killed and offspring do not survive long outside the womb. The study of embryonic development is easier in birds than in mammals, because the avian embryo can be continuously viewed over hours and days both in the shell and in artificial culture systems. Current techniques for *in vivo* imaging in chick embryos require the injection of dyes or electroporation of plasmids (26), but these invasive techniques can disrupt normal development. Transgenic or mosaic birds could offer a powerful advantage in experiments where current methods of cell labeling cannot be used.

We anticipate that avian transgenesis would be particularly useful for the study of behavioral neurobiology. Experiments with transgenic, mutant, and knock-out mice have been extremely valuable in studying the molecular basis of instinctual behavior as well as learning and memory (27). However, for the study of many behaviors, avian species are the preferred model organisms. Avian species exhibit a wide range of well studied behaviors, such as food hoarding (28), filial imprinting (29), sound localization (30), and vocal learning (31). Transgenesis with lentiviral vectors will allow for the precise molecular dissection of these behaviors.

In addition to its use in basic science research, avian transgenesis has potential commercial applications, specifically in the production of therapeutic proteins. Transgenic birds generated by using oncoretroviral vectors have been shown to express low levels of transgene in the egg whites of laid eggs (32). The chicken ovalbumin promoter has been suggested as a regulatory sequence for directing protein expression in egg whites (33). Using lentiviral vectors containing the ovalbumin promoter, transgenic chickens could be engineered to produce high levels of therapeutic protein in their egg whites, providing a high-yield source of biopharmaceuticals.

In summary, we have developed a method for the generation of transgenic animals with tissue-specific expression in a group of species for which genetic experiments were previously not feasible. Although birds have historically been useful for studying many important problems in development and neurobiology (34, 35), research in mice (and in other animals in which genetic and molecular experiments are possible) has dominated these fields. However, for many questions in biology, avian species remain the model organisms of choice. We anticipate that lentiviral transgenesis will greatly improve our ability to study these questions and will be an asset to the growing field of avian genetics (36).

B.B.S. thanks A. Stolfi for assistance with egg injections and H. Y. Chung and L. Smith for help with figures.

1. Jaenisch, R. (1988) *Science* **240,** 1468–1474.
2. Sang, H. (2004) *Mech. Dev.* **121,** 1179–1186.
3. Bosselman, R. A., Hsu, R. Y., Boggs, T., Hu, S., Bruszewski, J., Ou, S., Kozar, L., Martin, F., Green, C., Jacobsen, F., *et al.* (1989) *Science* **243,** 533–535.
4. Mozdziak, P. E., Borwornpinyo, S., McCoy, D. W. & Petitte, J. N. (2003) *Dev. Dyn.* **226,** 439–445.
5. Harvey, A. J., Speksnijder, G., Baugh, L. R., Morris, J. A. & Ivarie, R. (2002) *Poultry Sci.* **81,** 202–212.
6. Mizuarai, S., Ono, K., Yamaguchi, K., Nishijima, K., Kamihira, M. & Iijima, S. (2001) *Biochem. Biophys. Res. Commun.* **286,** 456–463.
7. Lois, C., Hong, E. J., Pease, S., Brown, E. J. & Baltimore, D. (2002) *Science* **295,** 868–872.
8. Hofmann, A., Kessler, B., Ewerling, S., Weppert, M., Vogg, B., Ludwig, H., Stojkovic, M., Boelhauve, M., Brem, G., Wolf, E. & Pfeifer, A. (2003) *EMBO Rep.* **4,** 1054–1060.
9. Hofmann, A., Zakhartchenko, V., Weppert, M., Sebald, H., Wenigerkind, H., Brem, G., Wolf, E. & Pfeifer, A. (2004) *Biol. Reprod.* **71,** 405–409.
10. McGrew, M. J., Sherman, A., Ellard, F. M., Lillico, S. G., Gilhooley, H. J., Kingsman, A. J., Mitrophanous, K. A. & Sang, H. (2004) *EMBO Rep.* **5,** 728–733.
11. Chapman, S. C., Lawson, A., Macarthur, W. C., Wiese, R. J., Loechel, R. H., Burgos-Trinidad, M., Wakefield, J. K., Ramabhadran, R., Mauch, T. J. & Schoenwolf, G. C. (2005) *Development* **132,** 935–940.
12. Bellairs, R. & Osmond, M. (1998) *The Atlas of Chick Development* (Academic, San Diego).
13. Sambrook, J. & Russel, D. W. (2001) *Molecular Cloning: A Laboratory Manual* (Cold Spring Harbor Lab. Press, Woodbury, NY).
14. Plateroti, M., Vignoli, A. L., Biagioni, S., Di Stasi, A. M., Petrucci, T. C. & Augusti-Tocco, G. (1994) *J. Neurosci. Res.* **39,** 535–544.
15. Kioussis, D. & Festenstein, R. (1997) *Curr. Opin. Genet. Dev.* **7,** 614–619.
16. Mullen, R. J., Buck, C. R. & Smith, A. M. (1992) *Development* **116,** 201–211.
17. Thiel, G., Greengard, P. & Sudhof, T. C. (1991) *Proc. Natl. Acad. Sci. USA* **88,** 3431–3435.
18. Sauerwald, A., Hoesche, C., Oschwald, R. & Kilimann, M. W. (1990) *J. Biol. Chem.* **265,** 14932–14937.
19. Schoch, S., Cibelli, G. & Thiel, G. (1996) *J. Biol. Chem.* **271,** 3317–3323.
20. Jahner, D., Stuhlmann, H., Stewart, C. L., Harbers, K., Lohler, J., Simon, I. & Jaenisch, R. (1982) *Nature* **298,** 623–628.
21. Miyoshi, H., Blomer, U., Takahashi, M., Gage, F. H. & Verma, I. M. (1998) *J. Virol.* **72,** 8150–8157.
22. Padgett, C. A. & Ivey, W. D. (1959) *Science* **129,** 267–268.
23. Herskowitz, I. (1987) *Nature* **329,** 219–222.
24. Tiscornia, G., Singer, O., Ikawa, M. & Verma, I. M. (2003) *Proc. Natl. Acad. Sci. USA* **100,** 1844–1848.
25. Feng, G., Mellor, R. H., Bernstein, M., Keller-Peck, C., Nguyen, Q. T., Wallace, M., Nerbonne, J. M., Lichtman, J. W. & Sanes, J. R. (2000) *Neuron* **28,** 41–51.
26. Niell, C. M. & Smith, S. J. (2004) *Annu. Rev. Physiol.* **66,** 771–798.
27. Chen, C. & Tonegawa, S. (1997) *Annu. Rev. Neurosci.* **20,** 157–184.
28. Clayton, N. S. & Dickinson, A. (1998) *Nature* **395,** 272–274.
29. Horn, G. (2004) *Nat. Rev. Neurosci.* **5,** 108–120.
30. Konishi, M. (2003) *Annu. Rev. Neurosci.* **26,** 31–55.
31. Nottebohm, F. (1999) in *The Design of Animal Communication*, eds. Hauser, M. D. & Konishi, M. (MIT Press, Cambridge), pp. 63–110.
32. Harvey, A. J., Speksnijder, G., Baugh, L. R., Morris, J. A. & Ivarie, R. (2002) *Nat. Biotechnol.* **20,** 396–399.
33. Ivarie, R. (2003) *Trends Biotechnol.* **21,** 14–19.
34. Konishi, M., Emlen, S. T., Ricklefs, R. E. & Wingfield, J. C. (1989) *Science* **246,** 465–472.
35. Stern, C. D. (2005) *Dev. Cell* **8,** 9–17.
36. Brown, W. R., Hubbard, S. J., Tickle, C. & Wilson, S. A. (2003) *Nat. Rev. Genet.* **4,** 87–98.